Contents

Chapter 1

Introduction

The system considered in this work is a pair of 1D superconductors connected with a Josephson junction. For all the discussion presented it's crucial for one of superconductors to be topological.

Topological superconductivity is a relatively fresh topic in physics. On the one hand it's connected to particle physics through the notion of Majorana fermion – the particle coinciding with its own antiparticle [1]. It appears not only in Standard model context [2–4] , but also as a state in solids [5–16]. Despite the difference between these entities, there is a clear analogy between majoranas in condensed matter and majoranas in particle physics [17, 18].

On the other hand topological superconductivity is of interest to quantum computation community as a platform to build fault tolerant quantum memory [6, 19–21]. Although significant difficulties have appeared on this way, the intention to realize this program is still strong and gives the motivation to build superconducting samples, which demonstrate signatures of nontrivial topology and presence of Majorana fermions [22–24].

The proposition of using superconducting wires as carriers of Majorana fermions came from a seminal work of Kitaev [6]. The key ingredient of this system was a p-wave superconductivity assumed to be present in a wire. It was shown, that under certain conditions the Majorana state can be present at the end of the wire. After some time other propositions [25, 26] appeared, based on seminconductor-superconductor heterostructures with s-wave superconductivity, external magnetic field and spin-orbit coupling. It was showed, that the sign of quantity $g = B - \sqrt{\Delta^2 + \mu^2}$ (where B is magnetic field, Δ is the absolute value of superconducting order parameter and μ is a chemical potential) can be used as a topological index, and a Majorana state will appear where the sign of g is changing.

The model, considered in this work is close to the ones used in [25, 26]. It consists of two superconducting wires connected with a tunnel junction. However instead of domain wall of the sign of g, a tunnel barrier between areas with $g > 0$ and $g < 0$ is introduced. This model is formulated in detail in chapter 2. The spectrum of this model and stationary supercurrent are studied in chapter 3 and the ionization of the Majorana state under small external oscillating voltage is considered in chapter 4. Chapter 5 stands for the discussion of obtained results and their possible experimental realization, while chapter 6 concludes the study.

Chapter 2

The model

The model studied here is mostly inspired by the works [25] and [26] with the main difference being the presence of a tunnel contact between the wires. As will be shown in subsequent chapters, the barrier doesn't affect the appearance of Majorana state, but has important consequences for other properties of the system. In this chapter the model itself is presented.

2.1 Problem statement

The system under consideration consists of two 1D s-wave superconducting wires connected with a tunnel junction. There is a strong spin-orbit coupling assumed to be present and external magnetic field is applied in the direction perpendicular to the wire. The Hamiltonian of the bulk of each wire, written in the Bogoliubov-de-Gennes formalism, is similar to the ones presented in [25] and [26]:

$$\mathcal{H} = \int dy \; \Psi^\dagger(y) H \Psi(y) \qquad \Psi = \begin{pmatrix} \psi_\uparrow \\ \psi_\downarrow \\ \psi_\downarrow^\dagger \\ -\psi_\uparrow^\dagger \end{pmatrix} \tag{2.1}$$

$$H = \left(\frac{p^2}{2m} - \mu_0 \right) \tau_z + u p \sigma_z \tau_z + B \sigma_x + \Delta \tau_\phi \tag{2.2}$$

Here σ_i and τ_i are Pauli matrices in spin and particle-hole subspaces respectively, $\tau_\phi = \tau_x \cos\phi - \tau_y \sin\phi$, with ϕ being the superconducting phase, μ_0 is a chemical potential, B is an external magnetic field, Δ is the absolute value of superconducting order parameter and u is spin-orbit coupling constant with the dimension of velocity. The wire is aligned along the y-axis, while the direction of the magnetic field coincides with x-axis. Note, that only one component of spin-orbit is nonzero due to 1D nature of the problem.

The tunnel junction is introduced by applying an external electrical field. Its potential profile $U(y)$ is presented on figure 2.1(a). Inside each wire the potential is assumed to be homogeneous, though its value can be different to the right and to the left of the junction. The junction itself is modeled by a sharp peak of the potential.

To take this into account one should include an additional term $U(y)\tau_z$ in (2.2). However

this term can be combined with the second term of by (2.2) by introducing an effective chemical potential $\mu(y) = \mu_0 - U(y)$ (see figure 2.1(b)). From now on all presence of the external field will be hidden in $\mu(y)$.

The superconducting phase ϕ in left and right wires, ϕ_L and ϕ_R, can also be different. The phase inside the barrier is undefined as $\Delta(y) = 0$ there.
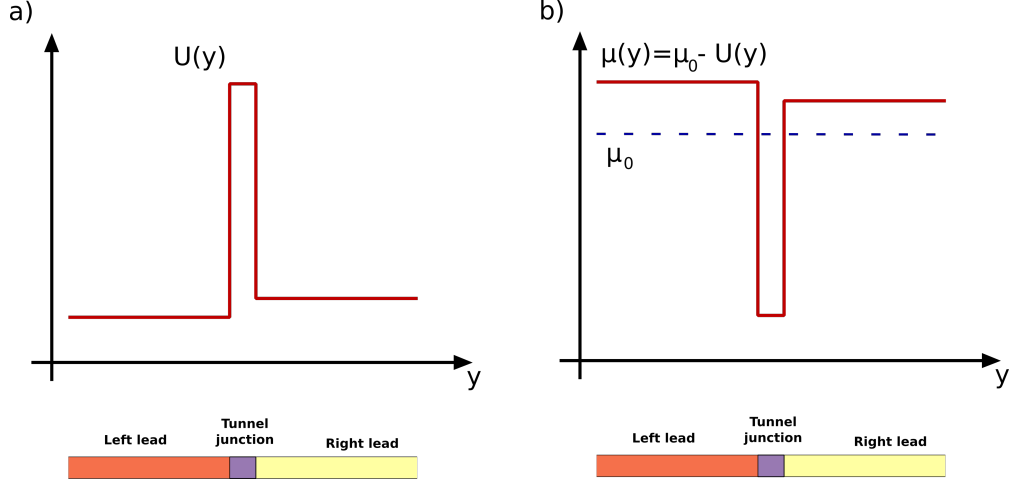
Figure 2.1: (a) y-profile of external electrical field. (b) y-profile of effective chemical potential

Finally, the BdG Hamiltonian for the model reads:

$$H = \left(\frac{p^2}{2m} - \mu(y) \right) \tau_z + u p \sigma_z \tau_z + B \sigma_x + \Delta(y) \tau_{\phi(y)} \tag{2.3}$$

with

$$\mu(y) = \begin{cases} \mu_L, & -\frac{L}{2} < y \\ \mu_b, & -\frac{L}{2} < y < \frac{L}{2} \\ \mu_R, & \frac{L}{2} < y \end{cases} \qquad \Delta(y) = \begin{cases} \Delta, & y > \frac{L}{2},\ y < -\frac{L}{2} \\ 0, & -\frac{L}{2} < y < \frac{L}{2} \end{cases} \tag{2.4}$$

$$\phi(y) = \begin{cases} \phi_L, & -\frac{L}{2} < y \\ \phi_R, & \frac{L}{2} < y \end{cases} \tag{2.5}$$

with L being the size of the junction. Note, that the parameters B, u, Δ and m are taken to be constant across the system.

This setup is close to one of the models considered by Oreg et al. in [25] ("*Spatially varying* μ" section). The difference is in the profile of $\mu(y)$ – in [25] there is a step in effective chemical potential, while here this function has a well.

In [25] it's also shown that the Majorana fermion appears at the interface between areas with different signs of the difference $B - \sqrt{\mu^2 + \Delta^2}$. As will be shown further, this is also relevant to

the system presented here. Note, that if $B > |\Delta|$ this condition can always be satisfied by choosing appropriate μ_L and μ_R.

When two wires of different sign of g are assumed in this work, the trivial wire will always be on the left, while the topological wire will always be on the right.

The model, described by (2.3) and (2.4) possesses a big number of external parameters. Different areas in this parameter space require different approaches and sometimes lead to completely different physics. Here certain experimentally reasonable constraints are assumed:

$$\mu_L, \mu_R \ll B \approx \Delta \ll mu^2 \ll |\mu_b| \tag{2.6}$$

The experimental justification of this choice is given in chapter 5. From the theoretical point of view the benefit of constraints $\mu_L, \mu_R \ll B \approx \Delta \ll mu^2$ is that they make it possible to use approximate wavefunctions in the wires. The inequality $mu^2 \ll |\mu_b|$ sets the system in the tunneling regime.

2.2   The dispersion of a homogeneous wire

Before discussing the properties of the junction it's necessary to consider a dispersion of a homogeneous wire modeled with the Hamiltonian (2.2). Although this can be done exactly, it's instructive to obtain this dependence step by step, starting with a simpler model and adding terms until the Hamiltonian (2.2) is restored.

The starting point is the Hamiltonian consisting only of kinetic energy and chemical potential terms: $H = \frac{p^2}{2m} - \mu$. It has simple parabolic dispersion presented on fig. 2.2(a). When the spin is introduced and spin-orbit coupling term $up\sigma_z$ is added, the parabola splits in two (fig. 2.2(b)), each one corresponding to its own z-projection of the spin. After introducing a magnetic field with $B\sigma_x$ term, the gap at the intersection opens (fig. 2.2(c)). The next step is introducing the BdG formalism, by adding the multiplier τ_z everywhere except for magnetic field term: $H = \left(\frac{p^2}{2m} - \mu_0\right)\tau_z + up\sigma_z\tau_z + B\sigma_x$. This procedure doubles the spectra in a way that each eigenvector with energy E obtains a partner eigenvector with energy $-E$, so two additional energy branches appear, being a mirror reflection of initial dispersion. This is presented on fig. 2.2(d), with the dashed lines being BdG partners. The last step is adding the superconducting term $\Delta\tau_\phi$, which opens the gap where dashed and solid lines intersect (fig. 2.2(e)).

As was mentioned before, the dispersion can be found explicitly. As was pointed out in [25], it can be done by squaring the Hamiltonian (2.2) twice and solving a resulting biquadratic

equation, leading to:

$$E_{1,2}^2(p) = B^2 + \Delta^2 + \xi_p^2 + (up)^2 \pm 2\sqrt{B^2\Delta^2 + B^2\xi_p^2 + (up)^2\xi_p^2} \qquad (2.7)$$

with $\xi_p = \frac{p^2}{2m} - \mu$. This dependence, presented on fig. 2.2(f), has two positive and two negative branches, as any BdG dispersion with electron-hole symmetry does. In further discussion only positive ($E > 0$) branches are considered, if opposite is not mentioned.
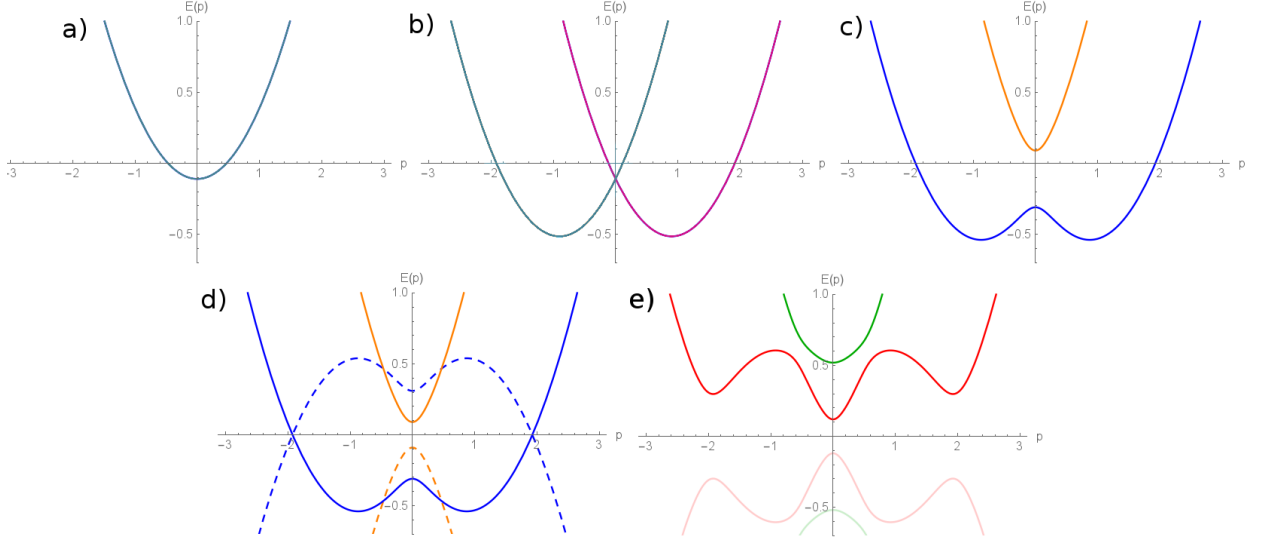

Figure 2.2: The dispersion of different Hamiltonians: a) mere kinetic energy and chemical potential: $H = \frac{p^2}{2m} - \mu$ b) spin-orbit coupling added: $H = \frac{p^2}{2m} - \mu_0 + up\sigma_z$ c) magnetic field added: $H = \frac{p^2}{2m} - \mu_0 + up\sigma_z + B\sigma_x$ d) BdG formalism introduced: $H = \left(\frac{p^2}{2m} - \mu_0\right)\tau_z + up\sigma_z\tau_z + B\sigma_x$ e) The complete Hamiltonian of homogeneous wire: $H = \left(\frac{p^2}{2m} - \mu_0\right)\tau_z + up\sigma_z\tau_z + B\sigma_x + \Delta\tau_\phi$. The parameters of the Hamiltonians for the plotting are: $B = 0.2$, $\Delta = 0.3$, $u = 0.9$, $m = 1$, $\mu = 0.11$

If the constrains (2.6) are assumed, the lower branch of this spectra has three minima: one of them is at $p = 0$ exactly, and two others are at $p = \pm 2mu$ in the leading order. The last two are not very interesting – the energy gap there is approximately equal to Δ, as it should be due to perturbative introduction of superconducting term. On the contrary, the minimum at $p = 0$, which is given by[25]:

$$E_2(0) = |g|, \quad g = B - \sqrt{\Delta^2 + \mu^2} \qquad (2.8)$$

is the most important peculiarity of the spectrum. First, as $\mu \ll B \approx \Delta$, it's the true gap of the spectrum as $\left|B^2 - \sqrt{\Delta^2 + \mu^2}\right| \approx \left|B - \Delta - \frac{\mu^2}{2\Delta}\right| \ll \Delta$. Second, the sign of g defines whether the wire host a Majorana state. Here it's useful to introduce the terminology: if $g > 0$ the wire is called "topological", otherwise it's called "trivial". In [25] and [26] it was derived, that the contact

of trivial and topological wire hosts a Majorana state. It can also be shown (see section 3.5.1), that this state is present at the end of a topological wire and isn't there for a trivial one.

Note, that when two wires are considered, there are two gaps, $g_{L,R} = B - \sqrt{\Delta^2 + \mu_{L,R}^2}$. When the magnetic field B is close to Δ, one can change the signs of $g_{L,R}$ by changing $\mu_{L,R}$ respectively.

For further discussion it's necessary to clarify the place of $g_{L,R}$ in the parameter hierarchy of the problem. To do so, we introduce $\beta = B - \Delta$. As $B \approx \Delta$, we find that $\beta \ll B, \Delta$. Recalling $\mu_{L,R} \ll B, \Delta$, one immediately finds that $g_{L,R} = B - \sqrt{\Delta^2 + \mu_{L,R}^2} \approx \beta - \frac{\mu_{L,R}^2}{2\Delta} \ll B, \Delta$.

2.3   Short-wave and long-wave wavefunctions

Though the wavefunctions of (2.2) can be found explicitly, their form is complicated enough to stall any further analysis. However, with the parameter hierarchy introduced in the previous section the Hamiltonian (2.2) can be treated perturbatively with the following strategy.

At first step only kinetic and spin-orbit terms are left in the Hamiltonian (2.2), so

$$H \approx \left(\frac{p^2}{2m} + up\sigma_z \right) \tau_z \tag{2.9}$$

As the presence of the Majorana state depends on sign of $g_{L,R}$, all the topological physics appears at the energies $E \sim g \ll mu^2$, so the energy term can also be omitted in Schroedinger equation . This leads to a couple of solutions for the momenta: $p_{\text{short}} \approx \pm 2mu$ and $p_{\text{long}} \approx 0$ with a corresponding wavefunctions — short-wave and long-wave ones.

Despite the fact that all the omitted terms in (2.9) are indeed smaller than the those retained, it can't be taken as zero order Hamiltonian — it's spectrum is ungapped, so all the solutions of Schroedinger equation are running waves and can't form a localized state. To introduce the gap one needs to add a superconductung term to (2.9). For short-wave ($p \approx 2mu$) wavefunctions this approximation is sufficient. These wavefuntions are treated in section 3.3.

For long-wave wavefunctions we can't add the superconducting term without adding a magnetic term, as they both significantly alter the momenta, and, consequentially, the wavefunctions. However, for this case the kinetic term, proportional to p^2, is much smaller than the spin-orbit term and thus can be omitted. The resulting Hamiltonian is similar to the ones used in [25, 26] and treated in section 3.4.

Chapter 3

Stationary properties

The stationary properties of the system are defined by its spectrum. In this chapter an effective boundary condition for long-wave wave functions is introduced, wavefunctions are obtained, sub-gap states are found and and the stationary supercurrent is investigated.

3.1 Boundary condition

To obtain the spectrum of the system it's necessary to find the wavefunctions inside the barrier. As the barrier chemical potential is the biggest energy parameter of the problem, they are defined by the Hamiltonian:

$$H(y) = \left(\frac{p^2}{2m} + \mu_b \right) \tau_z, \qquad -\frac{L}{2} < y < \frac{L}{2}. \tag{3.1}$$

As low energies are under consideration, in Schroedinger equation the energy term can be omitted, so $p_b \approx \pm i\sqrt{2m\mu_b}$. Matching the wavefunctions and their derivatives inside and outside the barrier, we take barrier wavefunctions out of the problem and obtain the following boundary condition for wavefunctions on the left and on the right of the barrier:

$$\begin{cases} \psi_L + b\partial_y\psi_L = t(\psi_R + b\partial_y\psi_R) \\ \psi_R - b\partial_y\psi_R = t(\psi_L - b\partial_y\psi_L) \end{cases} \tag{3.2}$$

where $\psi_{L,R} = \psi\left(\mp\frac{L}{2}\right)$, $b = (2m\mu_b)^{-\frac{1}{2}} = \frac{1}{p_b}$ — the penetration depth for the particle inside the barrier and $t = e^{-\frac{L}{b}}$ — the tunneling constant assumed to be small: $t \ll 1$. This condition means, that the size of the barrier L should be much bigger than the penetration depth b.

The condition (3.2) is invariant under the combined action $L \leftrightarrow R$, $y \to -y$. To simplify further analysis we reverse the direction in the left wire and shift both ends of the wires from $y = \frac{L}{2}$ to $y = 0$. The boundary condition than becomes:

$$\begin{cases} \psi_L - b\partial_y\psi_L = t(\psi_R + b\partial_y\psi_R) \\ \psi_R - b\partial_y\psi_R = t(\psi_L + b\partial_y\psi_L) \end{cases} \tag{3.3}$$

This transformation is illustrated on fig. 3.1. Note

The boundary condition (3.3) can be rewritten with the spinor $\Psi = (\psi_L, \psi_R)^T$ and Pauli matrices $\hat{s}_i$ in LR space:

$$(1 - t\hat{s}_x)\,\Psi - (1 + t\hat{s}_x)\,b\partial_y\psi = 0 \tag{3.4}$$

Since for all $t \neq 1$ (recall, that $t \ll 1$) the matrix is $1 \pm t\hat{s}_x$ in invertible multiplying the last equation by $(1 - t\hat{s}_x)/(1 + t^2)$ yields:

$$\left(1 - 2\tilde{t}\hat{s}_z - \tilde{b}\partial_y\right)\Psi = 0 \tag{3.5}$$

where $\tilde{t} = \frac{t}{1+t^2}$, $\tilde{b} = \frac{1-t^2}{1+t^2}b$. In the leading order in t, which corresponds to the tunneling limit, $\tilde{t} = t, \tilde{b} = b$.
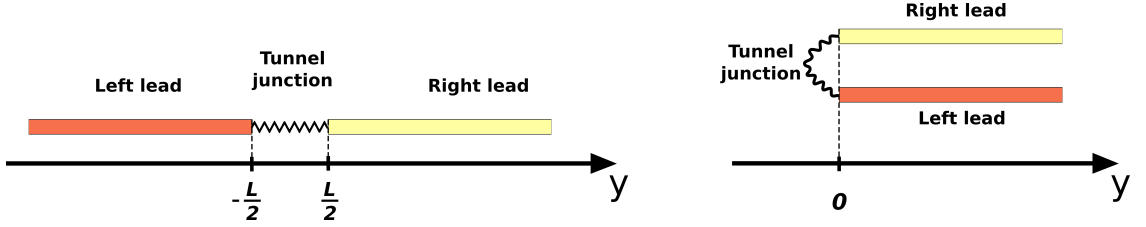
Figure 3.1: Illustration of switching the direction of left wire

One can argue that in tunneling limit the second and the third term in (3.5) are much smaller than the first one and should not be taken when the leading order is considered. However, if the second term is omitted, the wires become disconnected, and no tunnel effects can be found. The same is true for the third term — if it's not present, the boundary condition immediately implies $\Psi(0) = 0$, so the wires become disconnected again.

3.2   Short-wave wavefunctions

As was pointed in section 2.3, the short-wave wavefunctions should be described with the Hamiltonian (2.9) with a superconducting term:

$$H = \left(\frac{p^2}{2m} - up\hat{s}_z\sigma_z\right)\tau_z + \Delta\tau_\phi \tag{3.6}$$

here the multiplier $\hat{s}_z$ is added in the spin-orbit coupling term, as the direction of the left wire is inverted, so to write a correct Hamiltonian for LR space, one needs to change p to $-p$ for the left wire — which is adding $-\hat{s}_z$ multiplier to each momentum.

Denoting $\eta = \frac{p^2}{2m} - up\hat{s}_z\sigma_z$, one can rewrite (3.6) as $H = \eta\tau_z + \Delta\tau_\phi$. As $\hat{s}_z\sigma_z$ commutes

10

with H one can treat it as a number, so the dispersion is $E^2 = \eta^2 + \Delta^2$ (the number corresponding to eigenstate of $\hat{s}_z$ will be denoted as s_z while the number, corresponding to the eigenstate of σ_z will be denoted as ς_z). Thus $\eta = \pm i\sqrt{\Delta^2 - E^2}$, as the case $|E| < \Delta$ is assumed. For momenta one can write the equation:

$$p^2 - 2mus_z\varsigma_z p - 2m\eta = 0 \tag{3.7}$$

which for short-wave momenta gives $p_{\text{short}} \approx 2mus_z\varsigma_z + \frac{\eta}{u}s_z\varsigma_z$. Choosing the sign of η in a way, that the wavefunction decays at $x \to +\infty$, we obtain:

$$p_{\text{short}} \approx 2mus_z\varsigma_z + i\frac{\sqrt{\Delta^2 - E^2}}{u} \tag{3.8}$$

Now the wavefunction can be constructed by putting (3.8) into the Schroedinger equation $(\eta\tau_z + \Delta\tau_\phi)\Psi = E\Psi$. The solutions are:

$$\Psi_{s_z,\varsigma_z}(x) = \begin{pmatrix} 1 \\ e^{i(s_z\varsigma_z\gamma + \phi_{s_z})} \end{pmatrix}_{eh} e^{2imus_z\varsigma_z x - \frac{\sqrt{\Delta^2-E^2}}{u}x} |s_z, \varsigma_z\rangle \tag{3.9}$$

where $|s_z, \sigma_z\rangle$ are eigenvectors of $\hat{s}_z\sigma_z$, $\gamma = -\frac{\pi}{2} + \arcsin\frac{E}{\Delta}$ and $\phi_1 = \phi_L$, $\phi_{-1} = -\phi_R$ Thus the long-wave part the wavefunction can be written as:

$$\Psi_{\text{short}} = \sum_{s_z = \pm 1} \sum_{\varsigma_z = \pm 1} C_{s_z,\varsigma_z} \Psi_{s_z,\varsigma_z}(x) \tag{3.10}$$

3.3 Eliminating short-wave wavefunctions from boundary condition

As the Majorana state lives at low energies, it's expected to be predominantly long-wave. This argument is in accord with [25] and [26], where the Majorana state was an eigenstate of a linearized Hamiltonian, which is relevant only for long-wave physics. So, it's reasonable to eliminate the short-wave components from the problem, reformulating the boundary condition (3.5).

The wave function can be decomposed in short-wave and long-wave parts: $\Psi = \Psi_{\text{short}} + \Psi_{\text{long}}$. Inserting it into (2.9) and using the fact, that $p_{\text{long}} \ll p_{\text{short}} \approx 2mus_z\sigma_z$, one can obtain at the boundary:

$$(1 - 2t\hat{s}_x)\Psi_{\text{long}} + (1 - 2t\hat{s}_x - 2ibum\hat{s}_z\sigma_z)\Psi_{\text{short}} = 0 \tag{3.11}$$

Multiplying by the $(1 - 2t\hat{s}_x)^{-1}$ and omitting t^2 terms, we obtain:

$$\Psi_{\text{long}} = \left(-1 + i\zeta\left(1 + 2t\hat{s}_x\right)s_z\sigma_z\right)\Psi_{\text{short}} \tag{3.12}$$

with $\zeta = 2bum$.

Now, using the expansion (3.10) and renormalizing the coefficients: $C_{s_z\varsigma_z} \to -\left(1 - i\zeta s_z\varsigma_z\right)C_{s_z\varsigma_z}$ one can rewrite the boundary condition for ς_z spin component of the wavefunction as:

$$\Psi_{\text{long},\varsigma_z} = \left(1 + \frac{2i\zeta t\hat{s}_z\sigma_z}{1 + i\zeta\hat{s}_z\sigma_z}\right)\sum_{s_z=\pm 1}C_{s_z,\varsigma_z}\begin{pmatrix}1 \\ e^{i(s_z\varsigma_z\gamma + \phi_{s_z})}\end{pmatrix}_{eh}e^{2imus_z\varsigma_z x - \frac{\sqrt{\Delta^2 - E^2}}{u}x}|s_z, \varsigma_z\rangle \tag{3.13}$$

This can be multiplied by $\left(1 + \frac{2i\zeta t\hat{s}_z\sigma_z}{1 + i\zeta\hat{s}_z\sigma_z}\right)^{-1}$, which up to a t^2 correction yields:

$$\left(1 - \frac{2i\zeta t\hat{s}_z\sigma_z}{1 + i\zeta\hat{s}_z\sigma_z}\right)\Psi_{\text{long},\varsigma_z} = \sum_{s_z=\pm 1}C_{s_z,\varsigma_z}\begin{pmatrix}1 \\ e^{i(s_z\varsigma_z\gamma + \phi_{s_z})}\end{pmatrix}_{eh}e^{2imus_z\varsigma_z x - \frac{\sqrt{\Delta^2 - E^2}}{u}x}|s_z, \varsigma_z\rangle \tag{3.14}$$

For each ς_z the above equation can be interpreted as the requirement that the l.h.s. 4-vector (in LR- and eh-spaces) lies in the 2d linear space L_2 spanned by the the two vectors in the sum in the r.h.s.. This can be reformulated as the requirement that the l.h.s. be orthogonal to the complementary 2d space $\overline{L}_2$. There are two basic vectors $\overline{\Psi}_{s_z\varsigma_z}$ ($s_z = \pm 1$) spanning $\overline{L}_2$ for each ς_z:

$$\overline{\Psi}_{s_z\varsigma_z} = \begin{pmatrix}1 \\ -e^{i(s_z\varsigma_z\gamma + \phi_{s_z})}\end{pmatrix}|s_z, \varsigma_z\rangle \tag{3.15}$$

Thus one needs to multiply (3.14) by $\left(\overline{\Psi}_{+\varsigma_z}^T, \overline{\Psi}_{-\varsigma_z}^T\right)$ from the left and, after all evaluating the matrix product, find the effective boundary condition for long-wave wavefunctions in the form:

$$\begin{pmatrix}1 & -e^{-i(\varsigma_z\gamma - \phi_L)} & A & -Ae^{-i(\varsigma_z\gamma - \phi_L)} \\ A^* & -A^*e^{i(\varsigma_z\gamma + \phi_R)} & 1 & -e^{i(\varsigma_z\gamma + \phi_R)}\end{pmatrix}\Psi_{\text{long},\varsigma_z} = 0 \tag{3.16}$$

here $A = -\frac{2i\zeta t\varsigma_z}{1 + i\zeta\varsigma_z}$ and the elements are ordered as (Le, Lh, Re, Rh).

When studying wavefunctions in superconductors, it is more convenient to work with zero phase ϕ. This can be achieved by gauging the phase difference into the boundary condition. Indeed, suppose H_ϕ describes a wire with phase ϕ. Then, $H_\phi = U_\phi^\dagger H_0 U_\phi$ with $U_\phi = e^{-\frac{i\tau_z\phi}{2}}$ and the wave functions are also related via unitary rotation $\psi_\phi = U_\phi^\dagger\tilde{\psi}$. So the transform $\hat{U} = \text{diag}\left(U_{\phi_L}, U_{\phi_R}\right)_{L,R}$ will eliminate all the phases from the wires and put them into the boundary condition. Substituting $\Psi_{\text{long},\varsigma_z} = U^\dagger\tilde{\Psi}$ into (3.16) one arrives at an even simpler boundary condition on the zero-phase

function $\tilde{\Psi}$:

$$\begin{pmatrix} 1 & -e^{-i\varsigma_z\gamma} & A & -Ae^{-i(\varsigma_z\gamma+\varphi)} \\ A^* & -A^*e^{i(\varsigma_z\gamma+\varphi)} & 1 & -e^{i\varsigma_z\gamma} \end{pmatrix} \tilde{\Psi}_{\text{long},\varsigma_z} = 0 \tag{3.17}$$

where $\varphi = \phi_R - \phi_L$. Note, that any physical quantity can depend only on phase difference φ, but not on ϕ_L or ϕ_R separately.

It's also convenient to rewrite it in the form acting on the left and right wire wavefunctions:

$$M_L\tilde{\psi}^L_{\text{long}} + M_R\tilde{\psi}^R_{\text{long}} = 0$$

$$M_L = \begin{pmatrix} 1 & -e^{-i\sigma_z\gamma} \\ A^* & -A^*e^{i(\sigma_z\gamma+\varphi)} \end{pmatrix}_{eh} \qquad M_R = \begin{pmatrix} A & -Ae^{i(\sigma_z\gamma+\varphi)} \\ 1 & -e^{i\sigma_z\gamma} \end{pmatrix}_{eh} \tag{3.18}$$

This form is especially useful for finding subgap states localized near the barrier.

3.4 Low momenta and linearized Hamiltonian

To utilize boundary condition (3.16) or (3.17), it's necessary to find low momenta wavefunctions in homogeneous wire (this functions constitute ψ_{long} in (3.16) and (3.17). As was pointed in section 2.3, for this purpose one can use the linearized version of the Hamiltonian (2.2), like in [25] and [26]:

$$H = -\mu\tau_z + up\sigma_z\tau_z + B\sigma_x + \Delta\tau_x \tag{3.19}$$

here zero phase ϕ is assumed and μ is equal μ_L or μ_R depending on the wire considered. As was mentioned before, a nonzero phase can be restored by using U_ϕ matrix. This Hamiltonian is valid only for the right wire. To obtain the solution in the left wire one needs to reverse the sign of p in (2.2). Instead of doing so, the unitary transform $\psi_L = \sigma_x\psi_R$ can be utilized, as $H(-p) = \sigma_x H(p)\sigma_x$.

Remembering, that $\beta = B - \Delta \ll B, \Delta$, one can treat this Hamiltonian perturbatively and decompose it as $H = H_0 + V_0$:

$$H_0 = up\sigma_z\tau_z + \Delta(\sigma_x + \tau_x) \tag{3.20}$$

$$V = -\mu\tau_z + \beta\sigma_x \tag{3.21}$$

As H_0 commutes with $\sigma_x\tau_x$, it's convenient to rewrite it in the basis of common eigenstates

of σ_x and τ_x. Denoting them as $|\sigma_x, \tau_x\rangle$ and arranging the order as $(|+, +\rangle, |-, -\rangle, |+, -\rangle, |-, +\rangle)$ one can rewrite $H_0 + V$ as:

$$H_0 = \begin{pmatrix} 2\Delta & up & 0 & 0 \\ up & -2\Delta & 0 & 0 \\ 0 & 0 & 0 & up \\ 0 & 0 & up & 0 \end{pmatrix}, \qquad V = \begin{pmatrix} \beta & 0 & -\mu & 0 \\ 0 & -\beta & 0 & -\mu \\ -\mu & 0 & \beta & 0 \\ 0 & -\mu & 0 & -\beta \end{pmatrix} \qquad (3.22)$$

It's easy to see, that the wavefunctions from the subspace Span $(|+, +\rangle, |-, -\rangle)$ (we denote them as ψ_{medium}) require no perturbation to obtain the eigenstates in the leading order. Indeed, diagonalizing the upper subblock of H_0, one finds, that $E = \sqrt{(2\Delta)^2 + (up)^2}$. When the low energy states are the objects of interest ($E \sim g_{L,R}$), one finds, that $p = \pm\frac{i\Delta}{2u}$ in the leading order, and the corresponding wavefunctions are $|+, +\rangle \pm i |-, -\rangle$.

The other two eigenstates (we denote them as ψ_{longest}) are a little bit more complicated. Diagonalizing the lower subblock of H_0, one immediately finds, that $E = \pm up$. This corresponds to the fact, that H_0 is the version of H with a closed gap g on lower branch (see fig. 2.2,(e)), so in the zeroth order these states cannot form anything localized at all. To find them correctly, one needs to take into account the perturbation V and solve the secular equation using the following ansatz:

$$\psi = r_1 |+, +\rangle + r_2 |-, -\rangle + q_1 |+, -\rangle + q_2 |-, +\rangle \qquad (3.23)$$

with $r_i \ll q_j$ for all pairs (i, j). In the leading order (remember, that both E and up are of the order of $g_{L,R}$ now) this results in a couple of equations:

$$\begin{cases} \left(-E + B - \Delta - \frac{\mu^2}{2\Delta}\right) q_1 + upq_2 = 0 \\ upq_1 + \left(-E - B + \Delta + \frac{\mu^2}{2\Delta}\right) q_2 = 0 \end{cases} \qquad (3.24)$$

recall, that $g = B - \Delta - \frac{\mu^2}{2\Delta}$ and find $E^2 = g^2 + u^2 p^2$.

Now it's time to present these wavefunctions in original BdG basis. The expressions here are relevant only for the right wire and for $E > 0$. To find the wavefunctions in the left wire, the transform $\psi_L = \sigma_x \psi_R$ is used, while for finding the negative energy states we utilize electron-hole transform: $\psi_{E<0} = \tau_y \sigma_y K \psi_{E>0}$ with K being a complex conjugation operator.

For $E > 2\Delta$ wavefunctions ψ_{medium} are:

$$\psi_{\text{medium}}^{\text{out, in}}\bigg|_{E>2\Delta} = \begin{pmatrix} 1 \\ \frac{E \mp \sqrt{E^2 - 4\Delta^2}}{2\Delta} \\ \frac{E \mp \sqrt{E^2 - 4\Delta^2}}{2\Delta} \\ 1 \end{pmatrix} e^{\pm ix \frac{\sqrt{E^2 - 4\Delta^2}}{u}} \tag{3.25}$$

For $E < 2\Delta$ wavefunctions ψ_{medium} are

$$\psi_{\text{medium}}^{\text{grow, dec}}\bigg|_{E<2\Delta} = \begin{pmatrix} 1 \\ \frac{E \pm i\sqrt{4\Delta^2 - E^2}}{2\Delta} \\ \frac{E \pm i\sqrt{4\Delta^2 - E^2}}{2\Delta} \\ 1 \end{pmatrix} e^{\pm x \frac{\sqrt{4\Delta^2 - E^2}}{u}} \tag{3.26}$$

For $E > |g|$ wavefunctions ψ_{longest} are:

$$\psi_{\text{longest}}^{\text{out, in}}\bigg|_{E>g} = \begin{pmatrix} 1 \\ \frac{E \mp \sqrt{E^2 - g^2}}{g} \\ -\frac{E \mp \sqrt{E^2 - g^2}}{g} \\ -1 \end{pmatrix} e^{\pm \frac{ix\sqrt{E^2 - g^2}}{u}} \tag{3.27}$$

For $E < |g|$ wavefunctions ψ_{longest} are:

$$\psi_{\text{longest}}^{\text{grow, dec}}\bigg|_{E<g} = \begin{pmatrix} 1 \\ \frac{E \pm i\sqrt{g^2 - E^2}}{g} \\ -\frac{E \pm i\sqrt{g^2 - E^2}}{g} \\ -1 \end{pmatrix} e^{\pm \frac{x\sqrt{g^2 - E^2}}{u}} \tag{3.28}$$

3.5   Subgap states

To find the bound states one needs to make two linear combinations (each for its own wire) of decaying wave functions from (3.26) and (3.28) at $x = 0$ and put them into boundary condition (3.3). For the right wire they can be taken directly from (3.26) , (3.28), while for the left wire they should be multiplied by σ_x from the left (see the beginning of section 3.4).. These linear combinations can be written as:

$$\tilde{\psi}_L = C_{\text{medium}}^L \sigma_x \psi_{\text{medium}}^{\text{dec}} + C_{\text{longest}}^L \sigma_x \psi_{\text{longest}}^{\text{dec}} \qquad \tilde{\psi}_R = C_{\text{medium}}^R \psi_{\text{medium}}^{\text{dec}} + C_{\text{longest}}^R \psi_{\text{longest}}^{\text{dec}} \tag{3.29}$$

where $C^L_{\text{medium}}, C^L_{\text{longest}}, C^R_{\text{medium}}, C^R_{\text{longest}}$ are the undefined coefficients. Note, that the spinor $\psi^{\text{dec}}_{\text{medium}}$ is the same for the left and for the right wires.

Putting these combinations into boundary condition (3.3), we obtain four equations for these coefficients. If this system has a non-trivial solution at energy E_0, than there is a bound state with this energy. The condition of solvability can be written as:

$$\det F = 0 \tag{3.30}$$

where matrix F is given by:

$$F = \left(M_L \sigma_x \psi^{\text{dec}}_{\text{medium}}, \quad M_L \sigma_x \psi^{\text{dec}}_{\text{longest}} \quad M_R \psi^{\text{dec}}_{\text{medium}}, \quad M_R \psi^{\text{dec}}_{\text{longest}} \right) \tag{3.31}$$

As $E \sim g_{L,R} \ll \Delta$, the medium-wave spinor can be taken in its low-energy form: In most of this work the low energy version $\psi^{\text{dec}}_{\text{medium}} \approx (1, -i, -i, 1)^T$ will be sufficient.

For dealing with $\psi^{\text{dec}}_{\text{longest}}$ it is convenient to introduce two quantities $\chi_{L,R}$:

$$\cosh \chi_{L,R} = \frac{g_{L,R}}{\sqrt{g_{L,R}^2 - E^2}} \qquad \sinh \chi_{L,R} = \frac{E}{\sqrt{g_{L,R}^2 - E^2}} \tag{3.32}$$

If $g > 0$, the corresponding parameter χ is real and growing monotonously with E. For $g < 0$ the parameter χ is complex, but can be written as $\chi = -\tilde{\chi} + i\pi$ with real and monotonous $\tilde{\chi}$.

With these parameters the spinors $\psi^{\text{dec}}_{\text{L(R),longest}}$ at $x = 0$ can be written as:

$$\psi^{\text{dec}}_{\text{L(R),longest}} = \begin{pmatrix} -\sinh \chi_{L(R)} - i \\ -\cosh \chi_{L(R)} \\ \cosh \chi_{L(R)} \\ \sinh \chi_{L(R)} + i \end{pmatrix} \tag{3.33}$$

This parametrization completes the toolset used for studying the subgap spectrum.

3.5.1 The case of zero tunneling

Consider first equation (3.30) with $t = 0$. This corresponds to absolutely unpenetrable barrier, or, which is same, to independent wires ended with a vacuum. The computation of the determinant in (3.30) becomes a rather easy problem and results in:

$$\det F \Big|_{t=0} = -16 \left(i \sinh \left(\chi_L \right) + \cosh \left(\chi_L \right) - 1 \right) \left(i \sinh \left(\chi_R \right) + \cosh \left(\chi_R \right) - 1 \right) \tag{3.34}$$

If both g_L, g_R are negative (triv-triv junction), this determinant cannot be equal to zero at all, as $\cosh \chi_{L,R}$ are also negative and the real part in each bracket always non zero. If one of g_L, g_R (triv-top junction), say g_R, there is only one solution at $E = 0$. If both g_L, g_R(top-top junction) are positive, there are two solutions at $E = 0$.

This result proves, that the presence of Majorana mode in a isolated wire is defined only by the sign of g and justifies the notion of topology in this system.

3.5.2 Weak tunneling

To take into account the tunneling effect one may expand $\det F$ in t. Note, that there is no first order in t due to the structure of boundary condition (3.17). The decomposition can be written as:

$$\det F = d_0 + d_2 t^2 + \dots \tag{3.35}$$

where d_0 is given by (3.34). d_2 can be computed in a same way, but appears to be a rather complex formula. However, in tunneling limit the second term in (3.35) is small, so the only values of E that should be considered are the ones where d_0 is close to zero.

For triv-triv junction there are no such points, so in the tunneling limit there are no bound states for this case.

For triv-top junction there is a solution for $E = 0$, which corresponds to $\chi_L = i\pi$, $\chi_R = 0$. Computing d_2 for these parameters, one finds that it's exactly zero, so there is no correction to Majorana energy — as it should be, as this state protected by particle-hole symmetry. This solution with the first correction in t is presented in appendix A.

For top-top junction the situation is more interesting. In that case there are two solutions at $E = 0$, which should split for nonzero t. Calculating d_2 at $E = 0$ and expanding d_0 for small E, one finds:

$$d_0 = \frac{16E^2}{g_R g_L} \qquad d_2 = -\frac{256 t^2 \zeta^4}{(1 + \zeta^2)^2} \cos^2 \frac{\phi}{2} \tag{3.36}$$

Using, that $\zeta = 2bum \ll 1$, one can find the energy levels:

$$E_{1,2} = \pm 4t\zeta^2 \sqrt{g_R g_L} \cos \frac{\phi}{2} \tag{3.37}$$

this answer is relevant only if these level are well below the gaps: $t\zeta^2 \sqrt{g_R g_L} \ll \min [g_R, g_L]$.

3.6 Stationary supercurrent

The stationary supercurrent for a Josephson contact is given by [27]:

$$
I = -\frac{2e}{\hbar} \sum_p \tanh\left(\frac{\varepsilon_p}{2k_B T}\right) \frac{d\varepsilon_p}{d\varphi} -
$$

$$
-\frac{4e}{\hbar} k_B T \int\limits_{cont.} d\varepsilon \log\left[2\cosh\left(\frac{\varepsilon}{2k_B T}\right)\right] \frac{d\rho}{d\varphi} + \frac{2e}{\hbar} \frac{d}{d\varphi} \int dy \frac{|\Delta|^2}{|c|} \quad (3.38)
$$

Here ϵ_p are the energies of the states localized near the barrier, ρ is the density of states and $c(\mathbf{r})$ is the interaction constant of the BCS theory, φ is a phase difference, k_B is Boltzmann's constant and T is the temperature. The first term comes from the discrete spectrum and the sum is taken over all states in it, the second term is the current from continuous spectra and the third term comes from inhomogeneity of the order parameter. As pointed in [27], despite being generally nonzero, this last term doesn't contribute when step-model functions Δ like in (2.4) are used. The applicability of this approximation is a direct consequence of the tunneling regime considered in this work.

After omitting the third term and taking the low temperature limit one rewrites (3.38) as:

$$
I = -\frac{2e}{\hbar} \sum_p \frac{d\varepsilon_p}{d\varphi} - \frac{2e}{\hbar} \int\limits_{cont.} \varepsilon d\varepsilon \frac{d\rho}{d\varphi} \quad (3.39)
$$

As was shown in section 3.5, there are no subgap states in triv-top contact except Majorana state. But this state lies exactly at zero energy regardless of the phase difference, so the derivative in the first term of (3.39) will be zero and no supercurrent from the Majorana state is present.

To find the current from the continuous spectrum with (3.39) one needs to know the density of states. As there is a derivative over φ taken, one needs to find the phase dependent part of ρ only. It can be done by using the relation between the density of states and the scattering matrix [28]:

$$
\rho(\phi) = \frac{1}{2\pi i} \frac{\partial}{\partial \varepsilon} \log \det \hat{S} + const. \quad (3.40)
$$

The s-matrix connects the coefficients between the wavefunctions going to barrier and from it. It can be obtained with the help of wavefunctions (3.26), (3.25), (3.28) and (3.27) and boundary condition (3.3). To deal with radicals some additional parameters are used. When the given wavefunction is localized ($E < g$), θ-parametrization is used:

$$
\theta_{L,R}: \quad \sin\theta_{L,R} = \frac{E}{g_{L,R}}, \quad \cos\theta_{L,R} > 0 \quad (3.41)
$$

this parametrization is useful for both trivial and topological wires. When the wavefunction propagates ($E > g$), the η- or κ-parametrization is used, depending on the sign of g:

$$\eta_R : \quad \cosh \eta_R = \frac{E}{g_R}, \quad \sinh \eta_R > 0 \qquad \kappa_L : \quad \cosh \kappa_L = \frac{E}{|g_L|}, \quad \sinh \kappa_L > 0 \qquad (3.42)$$

To keep all the parameters real, η will be used for a topological wire, whereas κ will be used for a trivial wire. All the parameters $\theta_{L,R}$, κ_L and η_R are always real and positive when used.

As the dimension of s-matrix depends on the number of propagating modes, and thus on the energy, it's necessary to investigate different energy ranges separately.

For $E \ll \Delta$ one may use low energy limit of functions $\psi_{\text{medium}}^{\text{dec}}$: $\psi_{\text{medium}}^{\text{dec}} \approx (1, -i, -i, 1)^T e^{-\frac{2\Delta x}{u}}$ and also set $\gamma = -\frac{\pi}{2} \arcsin \frac{E}{\Delta} \approx -\frac{\pi}{2}$. When $E \sim \Delta$ one has to use γ as it is, and high energy of $\psi_{\text{longest}}^{\text{dec}}$: $\psi_{\text{longest}}^{\text{dec}} \approx (1, 0, 0, 1) e^{-\frac{Ex}{u}}$.

The eigenstates for the system at energies near g are presented in appendix A, in leading and subleading order on t. Here we focus on the result for the supercurrent in different cases.

3.6.1 Supercurrent for E between $|g_L|$ and g_R

Recall, that the trivial wire is placed on the left while the topological wire is on the right. There are two slightly distinct cases, which differ by relation between g_L and g_R.

The case $|g_L| > g_R$

For $g_R < E < |g_L|$ there is only one state wich goes towards the barrier, so the s-matrix has the dimension 1, and thus it's determinant coincides with it's only matrix element. The determinant which reads:

$$\det \hat{S} = -\frac{e^{\eta_R} + i}{1 + ie^{\eta_R}} - \frac{2i\zeta^4 t^2 e^{-i\varphi} \left(1 + e^{i\varphi}\right)^2 \left(-1 + e^{i\theta_L}\right) \left(e^{2\eta_R} - 1\right)}{\left(\zeta^2 + 1\right)^2 \left(1 + e^{i\theta_L}\right) \left(e^{\eta_R} - i\right)^2} + O\left(t^4\right) \qquad (3.43)$$

Using (3.39) (3.40), one finds, that:

$$I = \frac{8e}{\pi\hbar} t^2 \zeta^4 \sin \varphi \left(\sqrt{g_L^2 - g_R^2} - \int_{g_R}^{|g_L|} dE \frac{\sqrt{E^2 - g_R^2}}{\sqrt{1 - \frac{E^2}{g_L^2} + 1}} \right) \qquad (3.44)$$

It's easy to see, that $I \lesssim \frac{8e}{\pi\hbar} t^2 \zeta^4 g_R \sin \varphi$.

The case $|g_L| < g_R$

For $|g_L| < E < g_R$ the s-matrix (and its determinant) is:

$$\det \hat{S} = \frac{e^{\kappa_L} - i}{-1 + ie^{\kappa_L}} - \frac{2i\zeta^4 t^2 e^{-i\varphi} \left(1 + e^{i\varphi}\right)^2 \left(e^{2\kappa_L} - 1\right)\left(1 + e^{i\theta_R}\right)}{\left(\zeta^2 + 1\right)^2 \left(e^{\kappa_L} + i\right)^2 \left(-1 + e^{i\theta_R}\right)} + O\left(t^4\right) \tag{3.45}$$

Again with the help of (3.39) (3.40), one finds, that:

$$I = \frac{8e}{\pi\hbar} t^2 \zeta^4 \sin\varphi \left(\sqrt{g_R^2 - g_L^2} - g_R \int_{|g_L|}^{g_R} \frac{dE}{E^2} \sqrt{E^2 - g_L^2} \left(\sqrt{1 - \frac{E^2}{g_R^2}} + 1 \right) \right) \tag{3.46}$$

The estimate for this case is $I \lesssim \frac{8e}{\pi\hbar} t^2 \zeta^4 |g_L| \sin\varphi$.

3.6.2   Supercurrent for $|g_L|, g_R < E \ll \Delta$

In this case there are to states propagating towards the barrier – one in the right wire and one in the left, so the s-matrix is 2x2. Arranging its elements in the following order:

$$\hat{S} = \begin{pmatrix} r_{LL} & t_{LR} \\ t_{RL} & r_{RR} \end{pmatrix} \tag{3.47}$$

we find:

$$r_{LL} = \frac{e^{\kappa_L} - i}{-1 + ie^{\kappa_L}} + \frac{2\zeta^4 t^2 e^{-i\varphi}\left(1 + e^{i\varphi}\right)^2 \left(e^{2\kappa_L} - 1\right)\left(e^{\eta_R} + i\right)}{\left(\zeta^2 + 1\right)^2 \left(e^{\kappa_L} + i\right)^2 \left(-1 - ie^{\eta_R}\right)} + O\left(t^4\right) \tag{3.48}$$

$$r_{RR} = -\frac{e^{\eta_R} + i}{1 + ie^{\eta_R}} + \frac{2\zeta^4 t^2 e^{-i\varphi}\left(1 + e^{i\varphi}\right)^2 \left(e^{\kappa_L} - i\right)\left(e^{2\eta_R} - 1\right)}{\left(\zeta^2 + 1\right)^2 \left(-1 + ie^{\kappa_L}\right)\left(e^{\eta_R} - i\right)^2} + O\left(t^4\right) \tag{3.49}$$

$$t_{LR} = \frac{2\zeta^2 t e^{-i\varphi}\left(1 + e^{i\varphi}\right)\sqrt{\left(e^{2\kappa_L} - 1\right)\left(e^{2\eta_R} - 1\right)}}{\left(\zeta^2 + 1\right)\left(e^{\kappa_L} + i\right)\left(e^{\eta_R} - i\right)} + O\left(t^3\right) \tag{3.50}$$

$$t_{RL} = -\frac{2t\zeta^2\left(1 + e^{i\varphi}\right)\sqrt{\left(e^{2\kappa_L} - 1\right)\left(e^{2\eta_R} - 1\right)}}{\left(\zeta^2 + 1\right)\left(e^{\kappa_L} + i\right)\left(e^{\eta_R} - i\right)} + O\left(t^3\right) \tag{3.51}$$

The computation of supercurrent is again made with (3.39) (3.40). Introducing $g_{\max} = \max\left[g_R, |g_L|\right]$, $g_{\min} = \min\left[g_R, |g_L|\right]$ and

$$s_g = \begin{cases} 1, & g_R > |g_L| \\ -1, & g_R < |g_L| \end{cases} \tag{3.52}$$

one finds:

$$I = \frac{8e}{\pi \hbar} t^2 \zeta^4 \sin \varphi \left(s_g \sqrt{g_{\max}^2 - g_{\min}^2} - g_R \left| g_L \right| \int_{g_{\max}}^{\Delta} \frac{dE}{E^2} \left(\frac{\sqrt{E^2 - g_R^2}}{g_R} - \frac{\sqrt{E^2 - g_R^2}}{\left| g_L \right|} \right) \right) \quad (3.53)$$

It's important to note, that this computation is irrelevant for $E \sim \Delta$, so Δ here acts like hight energy cutoff. However the current from these states can be estimated as

$$I \sim \frac{e}{\hbar} t^2 \zeta^4 g_{\max} \log \left(\frac{\Delta}{g_{\max}} \right) \sin \varphi \quad (3.54)$$

3.6.3 Supercurrent for $\left| g_L \right|, g_R \ll E \lesssim \Delta$

To make the estimate for the supercurrent at energies $E \lesssim \Delta$ high energy limits of ψ_{longest} can be used, so the system "forgets" about g_L and g_R and becomes effectively symmetric. Taking the notation from (3.47), we find:

$$r_{LL} = r_{RR} = e^{i\gamma} +$$
$$+ \zeta^2 t^2 e^{-i\varphi} \left(\frac{(-1 + e^{2i\gamma})^2 (1 + e^{i\varphi})^2}{e^{i\vartheta} - e^{i\gamma}} + 2e^{i\gamma} \left(e^{2i(\gamma + \varphi)} + e^{2i\gamma} - 2e^{i\varphi} \right) \right) + O\left(t^4 \right) \quad (3.55)$$

$$t_{RL} = -t_{RL} = i\zeta t \left(1 + e^{2i\gamma} \right) \left(-1 + e^{i\varphi} \right) + O\left(t^3 \right) \quad (3.56)$$

where $\cos \vartheta = \frac{E}{2\Delta}$, $\sin \vartheta > 0$. Using (3.39) (3.40), we find:

$$I \sim \frac{e}{\hbar} \zeta^2 t^2 \Delta \sin \varphi. \quad (3.57)$$

3.6.4 Analyzing the results

From the estimates below (3.46) and (3.44) one may see, that the current coming from the states between g_L and g_R has a multiplier of the order g_R or $\left| g_L \right|$. The current from the states above $g_{\max}$ and near it can be estimated with (3.54). It has the multiplier $g_{\max} \log \frac{\Delta}{g_{\max}}$. Finally, according to (3.57), the current from the states near Δ is proportional to Δ. These results are schematically presented on fig. 3.2.
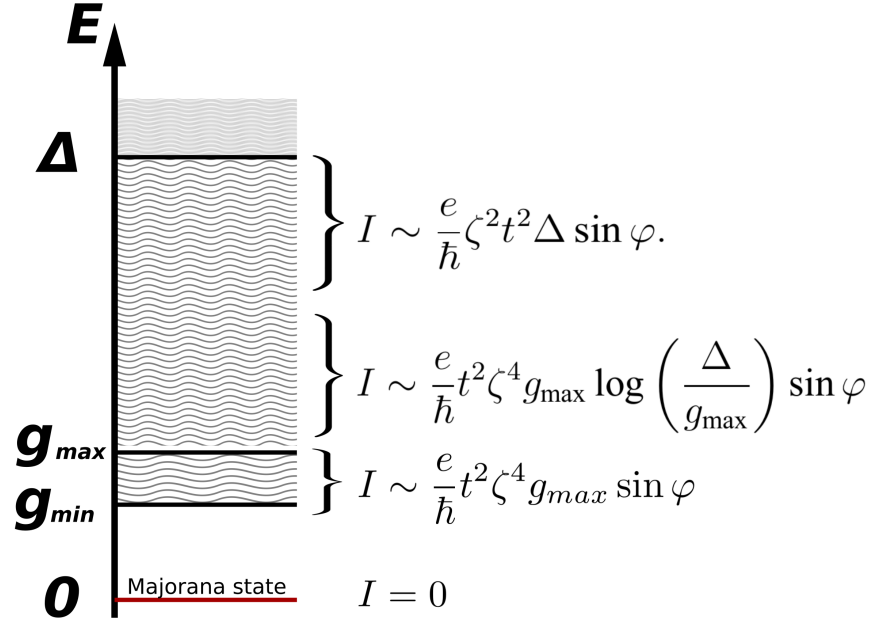
Figure 3.2: Supercurrent from different states

Thus we deduce that the current from the low energy states is negligible compared with the current from the states near Δ. This shows us that the low energy states ($E \ll \Delta$) contribute to stationary supercurrent by a very small quantity. The proportionality to Δ in (3.57) is similar to a conventional Josephson tunnel junction. We conclude, that measuring stationary supercurrent is unlikely to reveal any topological physics in this system.

Chapter 4

Ionization

In this chapter the model presented before is modified by introducing a small oscillating external voltage. This perturbation allows the Majorana state to excite into continuum — the process we will call ionization. The main goal here is to find the ionization rate when the typical size of the photon is much smaller than the spectrum gap. Only regime with $|g_L| \ll g_R$ is considered — this significantly simplifies the calculation, but still exhibits non-trivial physics with a number of different subregimes.

4.1 Introducing the perturbation

The perturbation is introduced as an oscillating voltage applied to the junction. This alters the Hamiltonian (2.3) in two ways — by the modification of the chemical potentials μ_L, μ_R and by making the superconducting phase difference $\varphi = \phi_R - \phi_L$ time dependent. The second effect is governed by the Josephson relation:

$$U(\tau) = \frac{\hbar}{2e} \frac{\partial \varphi(\tau)}{\partial \tau} \tag{4.1}$$

The ionization voltage is assumed to be small compared to other energy parameters, and this smallness is present in both effects. However, if the frequency ω of voltage is also small, the perturbation in Δ induced by the second effect will have additional big multiplier $\frac{\Delta}{\omega}$ and will dominate the perturbation in μ. In this chapter only this regime is considered.

Time dependence of phase difference is introduced as:

$$\varphi(\tau) = \varphi_0 + \alpha \cos \omega \tau \tag{4.2}$$

where φ_0 is an initial time independent phase difference and $\alpha \ll 1$ is the amplitude of phase oscillations.

As was shown in section 3.3, there is a gauge transform U_ϕ, which redistributes the phase difference between the wires, so the phase in a given wire can have any value. This ambiguity just reflects a fact, that only phase difference φ is an observable quantity, but not the phases ϕ_L, ϕ_R

separately. However, when treating the time dependent phase difference this gauge transform also becomes time-dependent. After its application the additional term $\dot{U}_{\phi(\tau)}U^\dagger_{\phi(\tau)} \propto \dot{\phi}(\tau)$ will appear, but, as ω is small, it can be neglected. The corresponding condition on ω is established in section 4.3.8.

As the term $\dot{U}_{\phi(\tau)}U^\dagger_{\phi(\tau)} \propto \dot{\phi}(\tau)$ is negligible, we again can gauge all the phase difference into the boundary condition. Now the boundary condition is time-dependent. It's not very convenient, and to avoid dealing with it we reformulate the problem in terms of tunnel Hamiltonian, which allow us to treat both tunneling and time dependence simultaneously via perturbation theory.

4.2   Tunnel Hamiltonian approach

The main idea of this method is to hide all the time dependence and the tunnel effect in one single operator. To do so we need to rewrite the Hamiltonian as $H = H_L + H_R + H_T$, where $H_{L,R}$ are the Hamiltonians of the left and right wire without any contact (corresponding to zero tunneling: $t = 0$), and H_T is a tunnel Hamiltonian both containing the time dependence and mixing the wavefunctions from different wires. Here the following notation is used: the Hamiltonians H_L, H_R and H_T are 8x8 matrices in combined Nambu-Gorkov and LR-space. In LR-space they have the following form:

$$H_L = \begin{pmatrix} h_L & 0 \\ 0 & 0 \end{pmatrix}_{LR} \qquad H_R = \begin{pmatrix} 0 & 0 \\ 0 & h_R \end{pmatrix}_{LR} \qquad H_T = \begin{pmatrix} 0 & h_{LR} \\ h_{RL} & 0 \end{pmatrix}_{LR} \tag{4.3}$$

The Hamiltonians h_L and h_R eventually coinside with (2.2) with zero boundary condition. The Hamiltonian $h_{LR} = h^\dagger_{Rl}$ in unknown — the goal is to make it in a way the corrections for the wavefunctions are restored . This wavefunctions and their first tunneling corrections are listed in appendix A.

The derivation of tunnel Hamiltonian matrix elements is presented in appendix B. Using the notation $\left| \gamma_0 \right\rangle$ for Majorana state and $\left| \varepsilon, L_0 \right\rangle, \left| \varepsilon, R_0 \right\rangle$ for continuous spectra, we have the following:

$$H_T = \left(e^{i\frac{\varphi}{2}} + e^{-i\frac{\varphi}{2}} \right) \tilde{H}_T = \left(e^{i\frac{\varphi}{2}} + e^{-i\frac{\varphi}{2}} \right) \begin{pmatrix} 0 & \tilde{h}_{LR} \\ \tilde{h}_{RL} & 0 \end{pmatrix} \tag{4.4}$$

$$\left\langle \gamma_0 \left| \tilde{h}_{RL} \right| E, L_0 \right\rangle = 4\sqrt{ug_R} t\zeta^2 f\left(\frac{E}{|g_L|} \right) \tag{4.5}$$

$$\left\langle \epsilon, R_0 \left| \tilde{h}_{RL} \right| E, L_0 \right\rangle = -16u\zeta^2 t f\left(\frac{E}{|g_L|} \right) f\left(\frac{\varepsilon}{g_R} \right) \tag{4.6}$$

where $f(x) = \sqrt{x^2 - 1}\left(x + \sqrt{x^2 - 1} \right)$.

The fact, that all energy dependences here are described by a single function $f(x)$ insinuates

that maybe it's possible to make this calculations in a more beautiful way.

4.3 Ionization rate for $g_R \gg |g_L|$

4.3.1 Time dependence of perturbation

To obtain the ionization rate one should treat H_T as perturbation. For unperturbed system, described with $H_0 = H_R + H_L$, the electrons cannot get from wire to another, but H_T allows these processes, so the ionization can be described as a set of jumps from right to left wire (see fig. 4.1).
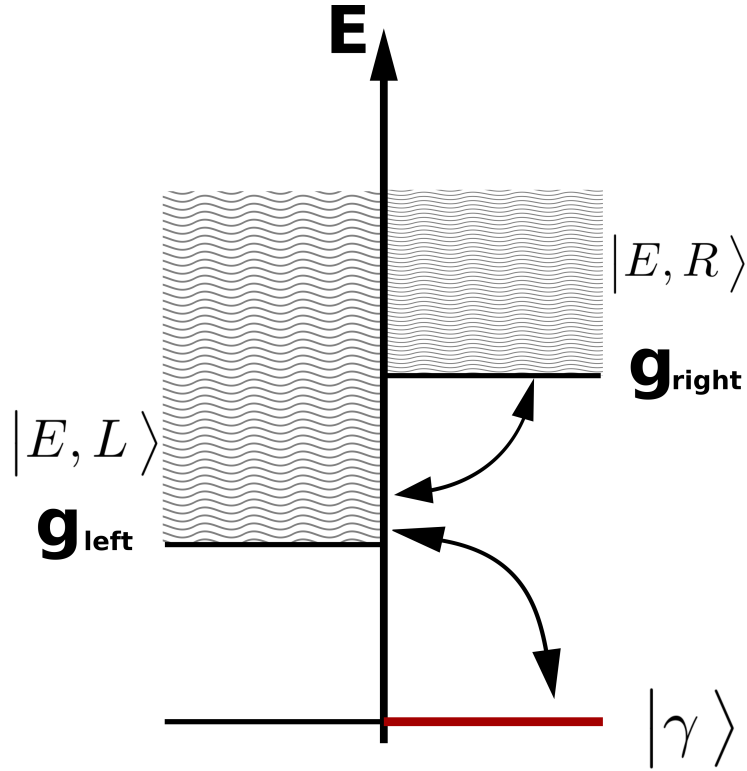

Figure 4.1: Ionization processes in terms of tunnel Hamiltonian

The approach to multiphoton ionization is described in Appendix C. The first step is to decompose the perturbation in Fourier series in frequencies. From (4.5) one finds, that $H_T \propto \cos\frac{\varphi(\tau)}{2}$ with $\varphi(\tau) = \varphi_0 + \alpha\cos\omega\tau$. Using $\alpha \ll 1$, we write:

$$e^{\frac{i\varphi(\tau)}{2}} + e^{-\frac{i\varphi(\tau)}{2}} \simeq e^{i\frac{\varphi_0}{2}} \sum_n \frac{(i\alpha)^n}{2^n n!}(e^{in\omega\tau} + e^{-in\omega\tau}) + c.c =$$

$$= \sum_n \frac{\alpha^n}{2^{2n-1}n!}(e^{in\omega\tau} + e^{-in\omega\tau})\cos\left(\frac{\varphi_0}{2} + n\frac{\pi}{2}\right) \quad (4.7)$$

so:

$$H_T = \sum_n H_{T,n} \left(e^{in\omega\tau} + e^{-in\omega\tau} \right), \qquad H_{T,n} \approx \sum_n \frac{\alpha^n}{2^{2n-1}n!} \cos\left(\frac{\varphi_0}{2} + n\frac{\pi}{2} \right) \tilde{H}_T \qquad (4.8)$$

The same decomposition is valid for LR matrix elements of H_T:

$$h_{LR} = \sum_n h_{LR,n} \left(e^{in\omega\tau} + e^{-in\omega\tau} \right), \qquad h_{LR,n} \approx \sum_n \frac{\alpha^n}{2^{2n-1}n!} \cos\left(\frac{\varphi_0}{2} + n\frac{\pi}{2} \right) \tilde{h}_{LR} \qquad (4.9)$$

Then the rate is given by (see Appendix C):

$$\mathcal{I} \sim \frac{|\langle \mathcal{E}|w_{\mathcal{E}}|\gamma \rangle|^2}{N_L(\mathcal{E})}, \qquad w_{\mathcal{E}}(E) = \sum_{\{n_i\}:\mathcal{E}} H_{T,n_N} \prod_{j=1}^{N-1} G_0 \left(E + \sum_{s=1}^{j} \omega_{n_s} \right) H_{T,n_j} \qquad (4.10)$$

here sum is taken over all sets $\{n_i\} : \mathcal{E}$ so that $\sum_i \omega_{n_i} = \mathcal{E} = \min[g_R, |g_L|]$. Each term in sum (4.10) corresponds to some way (i.e. trajectory) to absorb photons with energies ω_{n_i}, such that the total absorbed energy is equal to spectrum gap. Recall that Planck constant here is taken to be unity.

For unperturbed Green function we take a notaion:

$$G_0 (E) = \begin{pmatrix} G_L (E) & 0 \\ 0 & G_R (E) \end{pmatrix}_{LR}. \qquad (4.11)$$

In this section the focus is on the case where the topological gap is much larger than the trivial one: $|g_L| \ll g_R$. Then the right continuum has high energies and does not participate in the ionization process. Indeed,

$$h_{LR} G_R (\epsilon) h_{RL} = \frac{h_{LR}|\gamma\rangle\langle\gamma|h_{RL}}{\epsilon} + \int_{|E|>g_R} \frac{h_{LR}|E, R_0\rangle\langle E, R_0|h_{RL}}{\epsilon - E} \frac{dE}{N_R(E)} \qquad (4.12)$$

So, when $g_R \gg \epsilon \sim |g_L|$, the second term is small and can be neglected. Then, the product $\dots h_{RL} G_L (E) h_{LR} G_R (E) h_{RL} \dots$ factorizes into individual factors, which we denote as $J_{nm} (E) \equiv \langle\gamma|h_{RL,n} G_L (E) h_{LR,m}|\gamma\rangle$.

4.3.2 Factorizing $w_{\mathcal{E}}$

As each entry in the sum within $w_{\mathcal{E}}$ has the form $\dots h_{lR} G_R (E) h_{RL} G_L (E) h_{LR} \dots$, we have:

$$\sqrt{\mathcal{I}} \propto \sum_N \sum_{\{n_i\}_M^N} J_{n_1 n_2} J_{n_3 n_4} \cdots J_{n_{N-1} n_N} \qquad (4.13)$$

Here N has the meaning of total number of absorbed photons, M is the integer closest to $\frac{|g_L|}{\omega}$, and the second sum is taken over all sets $\{n_i\}_M^N$ of N items such that $\sum_{i=1}^N n_i = M$. We set, the number N to be even, hiding the last photon into unimportant prefactor.

The n,m-dependence factors out:

$$J_{nm}(E) = \frac{\alpha^{n+m}}{2^{2(n+m)-2}n!m!} \cos\left(\frac{\varphi_0}{2} + n\frac{\pi}{2}\right) \cos\left(\frac{\varphi_0}{2} + m\frac{\pi}{2}\right) Q_0(E) \tag{4.14}$$

$$Q_0(E) = \langle\gamma|\tilde{h}_{RL} G_L(E) \tilde{h}_{LR}|\gamma\rangle \equiv \int\limits_{cont.} \frac{|\langle\gamma|\tilde{h}_{LR}|\epsilon\rangle|^2}{E - \epsilon} \frac{d\epsilon}{N_L(\epsilon)} \tag{4.15}$$

On each ionization step the particle can move to the state with energy E or $-E$, so:

$$Q_0(E) = 2E \int\limits_{|g_L|}^{\infty} \frac{|\langle\gamma|\tilde{h}_{RL}|\epsilon\rangle|^2}{E^2 - \epsilon^2} \frac{d\epsilon}{N_L(\epsilon)} \tag{4.16}$$

recalling (4.5), we obtain:

$$Q_0(E) = ET \frac{\left[-1 + \sqrt{1 - \lambda^2}\right]}{\lambda^2} \tag{4.17}$$

where $\lambda = \frac{E}{|g_L|}$, $T = \frac{g_R(\zeta^2 t)^2}{|g_L|}$. We consider $T \ll 1$, so the systems remains in a strong tunneling limit.

Thus, the elementary block in our product for small enough E becomes:

$$\frac{J_{nm}}{E + n\omega} \approx \frac{J_{nm}}{E} = \left(\frac{\alpha}{4}\right)^{n+m} B_n B_m T \frac{-1 + \sqrt{1 - \lambda^2}}{\lambda^2} \tag{4.18}$$

where

$$B_n = \frac{2}{n!} \cos\left(\frac{\phi_0}{2} + \frac{\pi n}{2}\right) \tag{4.19}$$

The prefactor $(\alpha/4)^{n+m}$ yields $(\alpha/4)^{\mathcal{E}/\omega}$ for any trajectory and therefore do not affect summation and optimization. Thus one has $B_n B_m T \frac{-1+\sqrt{1-\lambda^2}}{\lambda^2}$ to optimize.

Now consider a slice of the ionization process, i.e. a part of the full ionization product, which runs from energy E to $E + \Delta E$ where $\Delta E = M\omega$ with a large M. One can assume that within that process, a large number N of photons is absorbed, but energy does not change significantly, $\Delta E \ll E$, so that λ can be considered a constant within that process.

This approach is invalid, if the optimal photon energy is larger than the slice size. If this happens, one needs to enlarge the slice until it reaches the energy of optimal photon. It cannot be

done, when the optimal photon energy is equal or larger than spectrum gap. This case is treated separately in section 4.3.6.

For now, denoting

$$T_\lambda = -4T \frac{\left[-1 + \sqrt{1 - \lambda^2}\right]}{\lambda^2} \tag{4.20}$$

we rewrite:

$$\mathcal{J}(\lambda) \equiv \sum_N \sum_{\{n\}_N^M} \frac{J_{n_1 n_2} J_{n_3 n_4} \cdots J_{n_{N-1} n_N}}{E^{\frac{N}{2}}} = \left(\frac{\alpha}{4}\right)^M \sum_N (-T_\lambda)^{\frac{N}{2}} \mathcal{J}_N \tag{4.21}$$

$$\mathcal{J}_N = \sum_{\{n\}_N^M} \prod_{i=1}^N \frac{\cos(\frac{\varphi_0}{2} + \frac{\pi n_{2i}}{2})}{n_i!} \tag{4.22}$$

So to obtain the ionization rate up to a prexponential constant, one should compute $\mathcal{J}(\lambda)$ and take the product $\prod_{\lambda_k} \mathcal{J}(\lambda_k)$ where λ_k corresponds for the k-th slice of the ionization process.

4.3.3 Estimation for optimal photon number

We begin dealing with (4.21) by finding the optimal photon number N_*. This number corresponds to the largest term in the sum (4.21).

The first step is to use Poisson summation formula:

$$\sum_{n=-\infty}^{\infty} \delta(x - n) = \sum_{k=-\infty}^{\infty} e^{2i\pi x} \tag{4.23}$$

so:

$$\mathcal{J}_N =$$

$$= \left(\sum_{k_1=-\infty}^{\infty} \cdots \sum_{k_{N-1}=-\infty}^{\infty}\right) \prod_{i=1}^{N-1} \left(\int dx_i e^{2i\pi k_i x_i} \frac{\cos\left(\frac{\varphi_0}{2} + \frac{\pi x_i}{2}\right)}{\Gamma(x_i + 1)}\right) \frac{\cos\left(\frac{\varphi_0}{2} + \frac{\pi x_N}{2}\right)}{\Gamma(x_N + 1)} \tag{4.24}$$

where $x_N \equiv M - \sum_{i=1}^{N-1} x_i$. This can be rewritten as:

$$\mathcal{J}_N = \frac{1}{2^N} \sum_{\mathbf{k}} \left(\sum_{s_1=\pm 1} \cdots \sum_{s_N=\pm 1}\right) \left(\prod_{i=1}^{N-1} \int dx_i\right) e^{S[\mathbf{x}]} \tag{4.25}$$

with

$$S[\mathbf{x}] = -\sum_{i=1}^{N} \log \Gamma\left(x_i + 1\right) + 2i\pi \sum_{i=1}^{N-1} k_i x_i + i \sum_{i=1}^{N} s_i \left(\frac{\varphi_0}{2} + \frac{\pi x_i}{2}\right) \qquad (4.26)$$

As N and M are large, we assume that x_i at saddle points are also large, so the Stirling approximation is relevant: $\log \Gamma\left(x\right) \approx x \log x - x$. As we just make the estimation for saddle point position, we can neglect all the terms in (4.26) except for the first one and get (recall, that $x_N = M - \sum_{i=1}^{N-1} x_i$):

$$\frac{\partial}{\partial x_i} S[\mathbf{x}] \approx \log x_N - \log x_i \qquad (4.27)$$

So, at the saddle point all x_i are equal to $\frac{M}{N}$.

Each x_i corresponds to it's own n_i. In saddle point approximation we can take only terms with $n_i = x_i^{\text{saddle}}$ in sum (4.22). Than the sum (4.21) becomes:

$$\mathcal{J}\left(\lambda\right) \approx \sum_N A_N \left(-T_\lambda\right)^{\frac{N}{2}} e^{-M \log \frac{M}{N}} = \sum_N A_N \left(-1\right)^{\frac{N}{2}} e^{\frac{N}{2} \log T_\lambda - M \log \frac{M}{N}} \qquad (4.28)$$

with relatively slow function A_N.

It's easy to see, that the biggest term in (4.26) corresponds to the $N_* = 2M / \log \frac{1}{T_\lambda}$. This is the optimal photon number for the slice from E to $E + \Delta E$ of energy range with $E = |g_L|\, \lambda$ and $\Delta E = \omega M$. Consequentially the optimal photon size is given by $n_* = \frac{M}{N_*} = \frac{1}{2} \log \frac{1}{T_\lambda}$. From (4.20) we see, that T_λ differs from T by a smooth depending on λ prefactor. We introduce a global optimal photon size $n_T \equiv \log \frac{1}{T} \gg 1$ and find, that $n_* \sim n_T$. It's important to note, that n_* doesn't depend on the energy slice size M, being an intensive parameter of the process.

4.3.4 Two regimes of factorized ionization

To treat (4.22) more accurately it's convenient to use the multinomial formula:

$$\frac{d^M}{dx^M} \prod_{i=1}^{N} f_i\left(x\right) = \sum_{\{n_i\}_N^M} \binom{M}{n_1, n_2, \ldots, n_N} \prod_{i=1}^{N} \frac{d^{n_i}}{dx^{n_i}} f_i \qquad (4.29)$$

For the cosine product it can be applied in a following way:

$$\sum_{\{n\}_N^M} \prod_{i=1}^{N} \frac{\cos(\chi + \frac{\pi n_i}{2})}{n_i!} = \sum_{\{n\}_N^M} \prod_{i=1}^{N} \frac{D_\chi^{n_i}}{n_i!} \cos \chi = \frac{1}{M!} D_\chi^M \cos^N \chi \qquad (4.30)$$

where $\chi = \frac{\varphi_0}{2}$. Then some algebra should be used:

$$\frac{1}{M!}D_\chi^M \cos^N \chi = \frac{1}{2^N M!}D_\chi^M \sum_{k=0}^{N} C_k^N e^{i\chi(N-2k)} = \frac{e^{i\chi N + iM\pi/2}}{2^N M!} \sum_{k=0}^{N} C_k^N (N-2k)^M e^{-2ki\chi} \quad (4.31)$$

So:

$$\mathcal{J}_N = \frac{e^{i\frac{\varphi_0}{2}N + iM\pi/2}}{2^N M!} \sum_{k=0}^{N} C_k^N (N-2k)^M e^{-ik\varphi_0} \quad (4.32)$$

Now, in the sum, the ratio of consecutive summands is $\frac{a_{k+1}}{a_k} = \frac{C_{k+1}^N}{C_k^N}\left(\frac{N-2k-2}{N-2k}\right)^M$. This ratio can be larger or less than unity. When $\frac{a_{k+1}}{a_k} < 1$ for any $k < \frac{N}{2}$, the largest ratio is $\frac{a_1}{a_0} = N\left(\frac{N-2}{N}\right)^M \simeq Ne^{-2M/N}$, so only a_0 and a_N should be taken into account. The summand $a_0 \propto e^{\frac{iN\varphi_0}{2}}$ corresponds to tunneling $N/2$ electrons to the left and $N/2$ holes to the right, while the $a_N \propto e^{\frac{-iN\varphi_0}{2}}$ corresponds to tunneling $N/2$ electrons to the right and $N/2$ holes to the left. So, the regime with only these two terms being present is a pure Andreev reflection regime. Taking $N = N_*$, we rewrite the condition $\left|\frac{a_1}{a_0}\right| \ll 1$ as $M \ll n_T e^{n_T} \sim T \log \frac{1}{T}$.

When this condition is broken, the largest terms in (4.32) are not a_0 and a_N. This corresponds to some mixture of Andreev and normal reflections and should be treated separately.

4.3.5   Pure Andreev reflection regime

In pure Andreev the sum (4.32) can be rewritten as:

$$\mathcal{J}(\lambda) \approx \left(\frac{\alpha}{4}\right)^M \sum_N (-T_\lambda)^{N/2} \frac{N^M}{2^{N-1}M!} \cos\left(\frac{N\varphi_0}{2} + \frac{M\pi}{2}\right) \quad (4.33)$$

The preexponent is not the object of interest, while the fixed parity of N should be taken into account. Here we set $N = 2K$. With the help of polylogarithmic function

$$\text{Li}_s(z) = \sum \frac{z^k}{k^s} \quad (4.34)$$

we rewrite (4.33) as:

$$\mathcal{J}(\lambda) = \left(\frac{\alpha}{4}\right)^M \sum_{K=1}^{\infty} (-T_\lambda)^K \frac{(2K)^M}{2^{2K-1}M!} \cos\left(\varphi_0 K + \frac{M\pi}{2}\right) =$$

$$= \frac{2}{M!}\left(\frac{\alpha}{4}\right)^M \Re\left[i^M \sum_K (-T_\lambda)^K \frac{(2K)^M}{2^{2K}} e^{i\varphi_0 K}\right] =$$

$$= \frac{2^{M+1}}{M!}\left(\frac{\alpha}{4}\right)^M \Re\left[i^M \text{Li}_{-M}\left(\frac{T_\lambda}{4} e^{i(\varphi_0 + \pi)}\right)\right] \quad (4.35)$$

30

The polylogarithmic function can be rewritten in the following useful way

$$\text{Li}_s(e^\mu) = \Gamma(1-s) \sum_{r \in \mathbb{Z}} (2r\pi i - \mu)^{s-1} \tag{4.36}$$

Substituting, we get

$$\text{Li}_{-M}\left(\frac{T_\lambda}{4} e^{i(\phi_0+\pi)}\right) = \Gamma(1+M) \sum_{r \in \mathbb{Z}} \left(i[2r\pi - \pi - \varphi_0] + \log \frac{4}{T_\lambda}\right)^{-M-1}$$

Denoting $\log \frac{4}{T_\lambda} = n_\lambda$ we have the ratio of consecutive terms in the sum (assuming they are not too far from the largest term):

$$\left|\frac{a_{r+1}}{a_r}\right| \sim \left(\frac{n_\lambda^2 + (\gamma_r + 2\pi)^2}{n_\lambda^2 + \gamma_r^2}\right)^{-1-M} \sim \left(1 + \frac{2\pi(2\pi + 2\gamma_r)}{n_\lambda^2 + \gamma_r^2}\right)^{-M} \sim \exp\left[\frac{4\pi M(\pi + \gamma_r)}{n_\lambda^2}\right]$$

where $\gamma_r = i(2r\pi - \pi - \varphi_0)$. There are two values of r for which $|\pi + \gamma_r|$ is smallest, for the rest it is not smaller than 2π so that the rest of the terms are smaller by at least $\exp\left[-\frac{8\pi^2 M}{n_\lambda^2}\right]$

This leads us to three additional subcases. When $M \gg n_\lambda^2 \sim n_T^2$, the sum over r is dominated by the largest terms: they correspond to $r = 0, 1$ for $-\pi < \varphi_0 < \pi$. The small number of terms in (4.36) corresponds to the large number of terms in (4.35), so in this case not only the trajectories with N_* contributes to ionization, but also the large number of neighboring ones.

When $M \ll n_\lambda^2$, the formula (4.36) isn't useful. Instead we look directly at (4.35) and find, that if $M < n_T$ only first term is relevant — which is single photon case, treated in section 4.3.6. When $n_T \ll M \ll n_T^2$, the maximum term in (4.35) is at $N_* \sim \frac{M}{n_T}$.

The subcases $n_T \ll M \ll n_T^2$ and $n_T^2 \ll M \ll n_T e^{n_T}$ are presented below.

Subcase $n_T^2 \ll M \ll n_T e^{2n_T}$

In this case we have

$$\text{Li}_{-M}\left(\frac{T_\lambda}{4} e^{i(\varphi_0+\pi)}\right) \simeq M! \left(\frac{1}{(n_\lambda + i(\pi - \varphi_0))^{M+1}} + \frac{1}{(n_\lambda + i(-\pi - \varphi_0))^{M+1}}\right) \tag{4.37}$$

For $\varphi_0 < 0$ only the first term should be left, while for the $\varphi_0 > 0$ only the the second one. Thus the answer, obviously, depends on φ_0 and can be obtained only for the case, say $\varphi_0 > 0$.

So we set:

$$\text{Li}_{-M}\left(\frac{T_\lambda}{4} e^{i(\varphi_0+\pi)}\right) \simeq \frac{M!}{(n_\lambda + i(\pi - \varphi_0))^{M+1}} \tag{4.38}$$

and:

$$\mathcal{J}(\lambda) = 2 \left(\frac{\alpha}{2}\right)^M \Re \left[\frac{i^M}{(n_\lambda + i(\pi - \phi_0))^{M+1}}\right] \tag{4.39}$$

Applying some algebra:

$$[n_\lambda + i(\pi - \phi_0)]^{M+1} = \left[n_\lambda^2 + (\pi - \phi_0)^2\right]^{\frac{M+1}{2}} e^{i(M+1)\arctan\frac{\pi-\phi_0}{n_\lambda}} \tag{4.40}$$

we find:

$$\mathcal{J}(\lambda) = 2 \left(\frac{\alpha}{2}\right)^M \frac{\cos\left(\frac{M\pi}{2} - (M+1)\arctan\frac{\pi-\varphi_0}{n_\lambda}\right)}{\left[n_\lambda^2 + (\pi - \phi_0)^2\right]^{\frac{M+1}{2}}} \tag{4.41}$$

This contains some complicated oscillations but within exponential accuracy we may write

$$\mathcal{J}(\lambda) \sim \exp M \left[\log\frac{\alpha}{2} - \frac{1}{2}\log(n_\lambda^2 + (\pi - |\varphi_0|)^2)\right] \tag{4.42}$$

The last thing to do is to take a product $\prod_{\lambda_k}\mathcal{J}(\lambda_k)$. It results to the integration of the quantity in the exponent over λ (the limits are 0 and 1 as $\lambda = \frac{E}{|g_L|}$):

$$s_\lambda = M\log\frac{\alpha}{2} - \frac{M}{2}\int_0^1 \log(n_\lambda^2 + (\pi - |\varphi_0|)^2)d\lambda \tag{4.43}$$

Calculation of the λ-integral:

$$\int_0^1 \log(n_\lambda^2 + (\pi - |\varphi_0|)^2)d\lambda \approx \int_0^1 \left(2\log n_\lambda + \frac{(\pi - |\varphi_0|)^2}{n_\lambda^2}\right)d\lambda \tag{4.44}$$

Separately we find (recall, that $n_T = \log\frac{1}{T}$):

$$\int_0^1 \log n_\lambda d\lambda \approx \log n_T + \frac{\pi - 2}{2n_T} - \frac{C_2}{n_T^2} + O\left(\frac{1}{n_T^3}\right). \tag{4.45}$$

where

$$C_2 = 2\int_0^1 d\lambda \left(\log\frac{\lambda^2}{1 - \sqrt{1 - \lambda^2}}\right) \approx 0.689 \tag{4.46}$$

The last integral in (4.44) is:

$$\int_0^1 \frac{1}{n_\lambda^2} d\lambda = \int_0^1 d\lambda \frac{1}{\left(n_T + \log \frac{\lambda^2}{1-\sqrt{1-\lambda^2}}\right)^2} = \frac{1}{n_T^2} + O\left(\frac{1}{n_T^3}\right) \tag{4.47}$$

Thus, we get

$$s_\lambda = \frac{2\,|g_L|}{\omega}\left(\log\frac{\alpha}{2} - \log n_T - \frac{\pi-2}{2n_T} + \frac{C_2}{n_T^2} - \frac{(\pi - |\varphi_0|)^2}{2n_T^2} + O\left(\frac{1}{n_T^3}\right)\right) \tag{4.48}$$

and the final result in this limit:

$$\mathcal{I} \propto \exp\left[-\frac{2\,|g_L|}{\omega}\left(\log\frac{2}{\alpha} + \log n_T + \frac{\pi-2}{2n_T} - \frac{C_2}{n_T^2} + \frac{(\pi - |\varphi_0|)^2}{2n_T^2} + O\left(\frac{1}{n_T^3}\right)\right)\right] \tag{4.49}$$

Subcase $n_T \ll M \ll n_T^2$

In this case the dominating term in (4.35) have large index K, but the gaussian envelope is very narrow, which means that the full series is dominated by a single term. This is in full agreement with the fact that the form (4.36) of polylogarithm converges over a large number of r-terms. The optimal term has the integer index K_0 closest to the real saddle-point $K_\lambda = M/n_\lambda$. We write $K_\lambda = K_0 + \xi_\lambda$, with $\xi_\lambda \in \left(-\frac{1}{2}, \frac{1}{2}\right)$, so:

$$\frac{1}{M!}\text{Li}_M\left(e^{-n_\lambda + i(\varphi_0 + \pi)}\right) \propto \frac{1}{M!}e^{-n_\lambda(K_\lambda - \xi_\lambda) + M\log(K_\lambda - \xi_\lambda)} = e^{-M\log n_\lambda - \frac{\xi_\lambda^2 n_\lambda^2}{2M} + O\left(\frac{n_\lambda^3}{M^2}\right)} \tag{4.50}$$

Here we have a nonlinear in M term. It means, that the answer for the ionization rate depends on how we split the process into energy slices. So, we must take only one slice — the whole gap. As we take only one slice, n_λ changes significantly inside it. Therefore the optimal photon number is not given by $\frac{M}{n_\lambda}$ anymore, and, consequentially, ξ_λ becomes ill-defined.

However, we can use the term $\frac{\xi_\lambda^2 n_\lambda}{2M}$ as an estimate for integer effects. It yields the following correction in the ionization exponent:

$$\mathcal{I} \propto \exp\left[-\frac{2\,|g_L|}{\omega}\left(\log\frac{2}{\alpha} - \log n_T - \frac{\pi-2}{2n_T}\right) + O\left(\frac{\omega n_T^2}{2\,|g_L|}\right)\right] \tag{4.51}$$

The linear term $\frac{|g_L|}{\omega}$ is obtained by averaging the action over λ as before. It isn't relate to integer effects and thus this procedure is legitimate.

4.3.6 Single photon case

When the optimal photon size is larger than the slice size ($n_T > M$), one again cannot use the procedure described in section 4.3.2 and divide the ionization process into pieces. In this case the system just takes one photon with the size of the gap and ionize. This case can be calculated exactly with conventional Fermi Golden rule (C.16) (with $N_L(E)$ in the denominator), where the perturbation is the term of (4.8) corresponding to the closest to $\frac{|g_L|}{\omega}$ larger integer. We denote this integer as M, consistent with the previous notation. The result is:

$$\mathcal{I} = \frac{\alpha^M}{2^{M-2}M!}t^2\zeta^4 g_R \cos\left(\frac{\varphi_0}{2} + \frac{\pi M}{2}\right)\frac{\sqrt{M^2\omega^2 - g_L^2}}{M\omega} \tag{4.52}$$

Note, that $M\omega$ is the actual energy of the destination state of the ionization. When $M\omega$ becomes equal to $|g_L|$, this expression gives zero. However, when this happens, the ionizing harmonic of H_T changes, so M switches to $M + 1$, and the result again becomes nontrivial.

4.3.7 Andreev+Normal reflection regime

Now consider the case $M \gg n_T \log n_T$ (or, which is the same, $M \ll N_* \log N_*$). In this case the sum (4.32) is not defined by the two edge terms. We write:

$$\sum_{k=0}^N C_k^N(N-2k)^M e^{-ik\varphi_0} = \sum_{k=0}^N e^{-S_0(k)-ik\varphi_0} \tag{4.53}$$

where the action S_0 is

$$S_0 = -\log C_k^N - M\log(N-2k) =$$
$$= -N\log N + k\log k + (N-k)\log(N-k)-$$
$$- M\log(N-2k) - \frac{1}{2}\log\frac{N}{2\pi(N-k)k} + \ldots \tag{4.54}$$

The stationary point of that action obeys $\partial S_0/\partial k = 0$:

$$\log k - \log(N-k) + \frac{2M}{N-2k} + \frac{1}{2k} - \frac{1}{2(N-k)} = 0 \tag{4.55}$$

As expected, $k \to N - k$ changes the sign of this. We seek for the stationary point with $k < N/2$. We have the transcendent equation (terms $\sim 1/k, 1/N$ are neglected)

$$\log\left(\frac{N}{k} - 1\right) = \frac{2M/N}{1 - 2k/N} \tag{4.56}$$

This is generally unsolvable, but if we assume that $M/N \gg 1$ then we get $k/N \ll 1$ and the asymptotic is

$$k_0 = Ne^{-2M/N} \tag{4.57}$$

We remind that this happens in the regimes $1 \ll M/N \ll \ln N$. At the same time, to have $k \gg 1$ produces the additional constraint $M/N \ll \frac{1}{2} \ln N$. At this saddle point, $k = k_0$, we have

$$\frac{\partial^2 S_0}{\partial k^2} \approx \frac{1}{k} + \frac{1}{N-k} + \frac{4M}{(N-2k)^2} \approx \frac{1}{k_0} + \frac{4M}{N^2} = \frac{1}{N}\left(e^{2M/N} + \frac{4M}{N}\right) \approx \frac{1}{k_0} \tag{4.58}$$

where we made use of $M/N \gg 1$. The action itself is:

$$S_0 = -M \log N + O\left(k_0 \log N\right) \tag{4.59}$$

We now integrate using the Poisson formula:

$$\sum_{k=0}^{N/2} e^{-S_0(k)-ik\varphi_0} = \sum_{p\in\mathbb{Z}} e^{-S_0(k_0)-ik_0(\varphi_0-2\pi p)} \int dk e^{-\frac{1}{2k_0}(k-k_0)^2-i(k-k_0)(\varphi_0-2\pi p)} =$$

$$= \sum_{p\in\mathbb{Z}} \sqrt{2\pi k_0} e^{-S_0(k_0)-ik_0(\varphi_0-2\pi p)-2(\frac{\varphi_0}{2}-\pi p)^2 k_0} \tag{4.60}$$

Assuming φ_0 is not close to $\pm\pi$ the above is dominated by the term with $p = 0$ because $k_0 \gg 1$. If we are close to π phase difference, there are two main terms, but, to an exponential accuracy the answer is still the same. In the above, we only integrated near the saddle-point with $k_0 < N/2$, there remains the symmetric saddle at $N - k_0$. This adds the complex conjugate to the result (but first we must restore some prefactors):

$$\frac{i^M e^{i\chi N}}{M! 2^N} \sum_{k=0}^{N} C_k^N (N-2k)^M e^{-2ki\chi} = 2\frac{\sqrt{2\pi k_0}}{M! 2^N} e^{-S_0-2\chi^2 k_0} \cos\left[-\frac{2k_0\varphi_0}{2} + \frac{N\varphi_0}{2} N \frac{M\pi}{2}\right] \tag{4.61}$$

The next step is to sum this over N. Remember that $k_0 = Ne^{-2M/N}$ and $S_0 = S_0(M, N, k_0(M, N))$.

Up to the preexponent we have:

$$\mathcal{J} \propto \Re \frac{i^M}{M!} \left(\frac{\alpha}{4}\right)^M \sum_N \left(-\frac{T_\lambda}{4}\right)^{N/2} \sqrt{k_0} e^{-S_0-\frac{\varphi_0^2}{4}k_0+i\frac{\varphi_0}{2}(N-2k_0)} \tag{4.62}$$

We drop the terms proportional to k_0 from the action as they are beyond our accuracy.

Recalling, that $N = 2K$, we write:

$$\mathcal{J} \propto \frac{1}{M!} \left(\frac{\alpha}{4} \right)^M \Re \left[i^M \sum_N \left(-\frac{T_\lambda}{4} \right)^K e^{-S_0 + i\varphi_0 K} \right] \quad (4.63)$$

This contains the same polylogaritm as in (4.35). As $M \gg n_T e^{n_T}$, we should treat it exactly as in the first subcase of the section 4.3.5. Thus we can just take the answer (4.49), but add an additional correction:

$$\mathcal{I} \propto \exp \left[-\frac{2|g_L|}{\omega} \left(\log \frac{2}{\alpha} + \log n_T + \frac{\pi - 2}{2n_T} - \frac{C_2}{n_T^2} + \frac{(\pi - |\varphi_0|)^2}{2n_T^2} + O\left(\frac{1}{n_T^3} \right) \right) + \right.$$
$$\left. + O\left(\frac{|g_L|}{\omega n_T} e^{-n_T} \log \frac{|g_L|}{\omega} \right) \right] \quad (4.64)$$

This correction comes from (4.59). At large enough $\frac{|g_L|}{\omega}$ it can become the greatest term in the exponent. This means, that in this case the approximation taken in (4.59) is insufficient.

4.3.8 The adiabaticity condition

In section (3.6) we gauged the time-dependent phase difference into H_T. This transformation generated the terms $\dot{U}U^\dagger = \dot{\varphi}\tau_z$ in the wires, and these terms were neglected.This approach in valid, when the ionization from the terms $\dot{\varphi}\tau_z$ is weaker than than the ionization from H_T.

To estimate the ionization caused by $\dot{\varphi}\tau_z$ we turn off the tunneling and look at the transitions in left and right wire separately.

In the left wire the transitions are possible only between the states of continuous spectrum. As $\dot{\varphi}\tau_z$. is homogeneous, the jumps are possible only between the states with equal momenta. From each state $|E, L_0\rangle$ with $E \sim |g_L|$ the transitions are possible only to the state $|-E, L_0\rangle$ and into two another states with energies of the order of Δ.

The matrix element $\langle E, L_0 | \tau_z | -E', L_0 \rangle \sim \frac{E}{\Delta} N_L(E) \delta(E - E')$. The smallness $\frac{E}{\Delta}$ occurs, as low energy states in leading order are eigenstates of the same eigenvalue of $\sigma_x \tau_x$, which anticommutes with τ_z. The matrix element $\langle E, L_0 | \tau_z | E_2, L_0 \rangle$ (with $E_2 \sim \Delta$) is proportional to $N_L \delta(E - E_2)$. Therefore the basic block $\langle E_0 | \dot{\varphi}\tau_z G \dot{\varphi}\tau_z | E_0 \rangle$ of the ionization process is proportional to $\frac{\omega^2 |g_L|}{\Delta^2}$. This should be compared with $\langle \gamma | H_T G H_T | \gamma \rangle$, which is given by the formula (4.17) and has the order $|g_L| T$. So, if $\omega \ll \Delta\sqrt{T}$, the adiabaticity holds.

Actually, the adiabaticity condition is even weaker, as $\dot{\varphi}$ has only the first harmonic in ω and therefore less efficient than H_T, which allows to optimize the photon size. The ionization with $\dot{\varphi}\tau_z$ always uses photons of the size ω and it scales as $e^{-M\left(\log \frac{1}{\alpha} + \log \frac{\Delta}{\omega} \right)}$. So, H_T prevails when the

condition

$$\omega \ll \frac{\Delta}{\log \frac{1}{T}} \tag{4.65}$$

holds.

The fact, that in adiabaticity condition ω is compared with Δ, not with $|g_L|$, means, that even the single photon limit from section 4.3.6 is achievable.

4.4 Results

Here we collect results for the ionization rate within exponential accuracy. We have the following notations: $T = \frac{g_R (\zeta^2 t)^2}{|g_L|} \ll 1$ — "dressed" tunneling constant relevant for the ionization, $M = |g_L| / \omega$ — the total number of energy quanta needed to ionize, $n_T = \log \frac{1}{T}$ – twice the optimal size of a photon (in quanta of ω). The optimal photon number is given by $N_* = \frac{2M}{n_T}$.
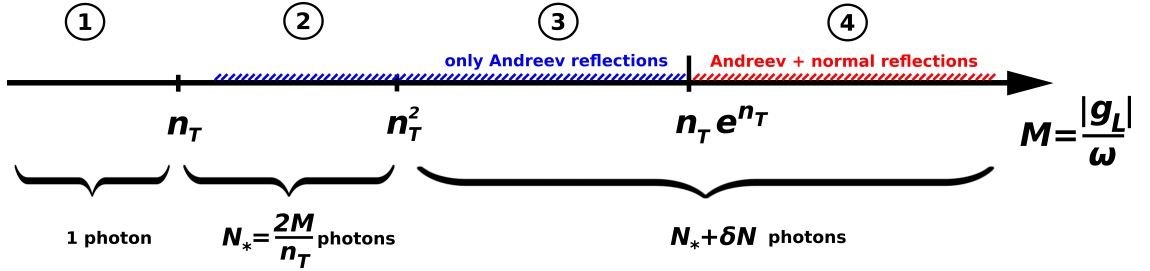

Figure 4.2: Different regimes of the ionization for $|g_L| \ll g_R$

There are four different regimes, which presented on fig.4.2 and given by the formulas (4.49), (4.51), (4.52) and (4.64). Here we list these results again:

1. Single-photon case: $M < n_T$. In this case, the tunneling parameter T is so small that it is best to use a single photon to minimize the $T^{N/2}$ factor in the amplitude J_{nm}. In this case the result (formula (4.52)) can be found even with the preexponent and yields:

$$\mathcal{I} = \frac{\alpha^M}{2^{M-2} M!} t^2 \zeta^4 g_R \cos\left(\frac{\varphi_0}{2} + \frac{\pi M}{2}\right) \frac{\sqrt{M^2 \omega^2 - g_L^2}}{M \omega} \tag{4.66}$$

2. Fixed number of photons case: $n_T \ll M \ll n_T^2$. In this case it is optimal to use multiple photons, more specifically $N_* = \frac{2M}{n_T}$ photons (rounded to the nearest integer). The contribution of the processes with different N is negligible. The integer effects are important here, but don't contribute in the leading terms. The ionization rate (formula (4.51)) is:

$$\mathcal{I} \propto \exp\left[-\frac{2|g_L|}{\omega}\left(\log\frac{2}{\alpha} - \log n_T - \frac{\pi - 2}{2 n_T}\right) + O\left(\frac{\omega n_T^2}{2|g_L|}\right)\right] \tag{4.67}$$

3. Fluctuating photon number case: $n_T^2 \ll M \ll n_T e^{n_T}$. Now, for combinatorial reasons, contributions from $N \neq N_*$ become important. The fluctuations $\delta N = N - N_*$ is typically much larger than unity but much smaller than N_*. Thus, no integer effects remain. We get (formula (4.49)):

$$\mathcal{I} \propto \exp\left[-\frac{2\,|g_L|}{\omega}\left(\log\frac{2}{\alpha} + \log n_T + \frac{\pi - 2}{2n_T} - \frac{C_2}{n_T^2} + \frac{(\pi - |\varphi_0|)^2}{2n_T^2} + O\left(\frac{1}{n_T^3}\right)\right)\right] \quad (4.68)$$

4. Mixed Andreev and normal reflections: $n_T e^{n_T} \ll M$. In this case there is an additional correction to the ionization rate, which can be even larger than leading term — in this case the result isn't valid. However, when this correction remains small, the ionization rate is (formula (4.64)) is:

$$\mathcal{I} \propto \exp\left[-\frac{2\,|g_L|}{\omega}\left(\log\frac{2}{\alpha} + \log n_T + \frac{\pi - 2}{2n_T} - \frac{C_2}{n_T^2} + \frac{(\pi - |\varphi_0|)^2}{2n_T^2} + O\left(\frac{1}{n_T^3}\right)\right) + \right.$$
$$\left. + O\left(\frac{|g_L|}{\omega n_T}e^{-n_T}\log\frac{|g_L|}{\omega}\right)\right] \quad (4.69)$$

These results are relevant, when the adiabaticity condition $\omega \ll \frac{\Delta}{\log\frac{1}{T}}$ discussed in section 4.3.8 holds.

Chapter 5

Discussion

In this chapter the obtained results are summarized and the potential experimental realization of the system is discussed.

5.0.1 Results summary

The results, obtained in chapters 3 and 4 has different potential for experiment realization. The subgap spectra can be obtained through the conductance measurements like was done in [22] and [24]. However as the conductance peak can be weakened by thermal broadening and scattering on the impurities, so it can be difficult to test that there are no states except for Majoranas – especially for the states near the gap. The results of chapter 3 tell, that measuring the system's supercurrent wouldn't be much different from the short Josephson junction problem.

However the ionization rates from the chapter 4 have a potential for experiment. Indeed, if the system has no Majorana state, the ionization rate will at least get an extra factor of 2 in the exponent in front of $\log \frac{2}{\alpha}$ term, as when there is no Majorana near the barrier, to make transition one needs to break a cooper pair and overcome the gap twice. It's unclear, whether the other corrections are observable — on the hand the all are multiplied by a large factor of $\frac{|g_L|}{\omega}$, on the other hand — they may be overshadowed by larger terms. Even the "large correctrion" $\log n_T = \log \log \frac{1}{T}$ has a double logarithm and may not be visible in real observation.

Despite all that, authors hope, that the obtained results can be used for developing techniques for detecting Majorana fermions in 1D superconducting wires. We also believe, that the analysis of the physics of this model can lead to deeper understanding of the processes taking place inside the superconducting wires with strong spin-orbit and external magnetic field and their Josephson contacts.

5.0.2 Possible experimental realization

The system, described in chapter 2, can be potentially be built in experimental setup similar to the ones used in [22] and [24].

The first problem, that seemingly makes all the work useless, is the fact that 1D superconductors don't exists due to the presence of fluctuations. However there is a bypass — one can make

superconducting wires artificially, taking a metallic or semiconducting wire and proximiting it to a strong superconductor. This is a well known method, used, for example, in [22] and [24].

The proposed setup for the system is presented on 5.1. A metallic or semiconducting wire (yellow) is being put on a insulator (gray) and proximitized to couple of superconductors (violet and cyan). It's important to make the superconductors separate, to obtain a phase difference and avoid shortcutting the barrier. The barrier itself can be created using a gate (red) with a big negative voltage on it. The chemical potentials in the wires can be adjusted in a similar way, by using a gates near each wire (green).
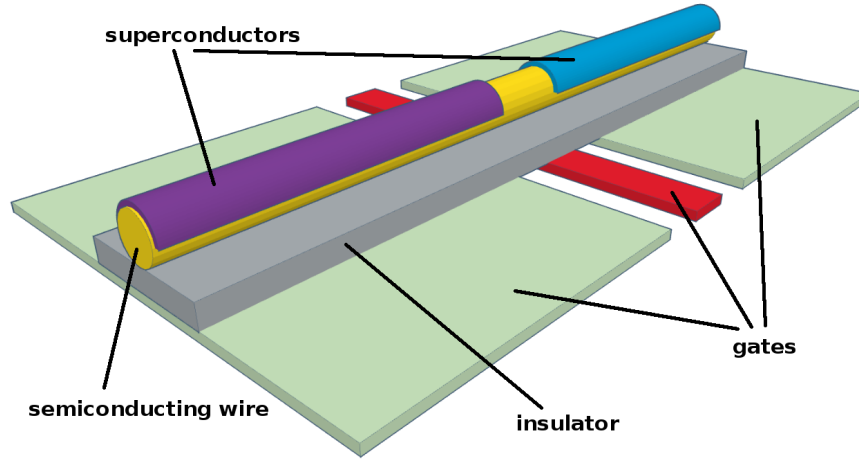

Figure 5.1: Possible experimental realization of the system

The procedure of adjusting the parameters of the model from the chapter 2 can be the following: at first the system is created, with superconductivity order parameter inside the wires being as similar, as possible. This may require a really advanced technique of fabricating the samples. After that the magnetic field B is turned on and being adjust to be a little larger than Δ. After that the gates should be set to switch the wires to desired topology and create a tunnel barrier.

When the model was chosen, it was considered that it's much easier to make spatially inhomogeneous electric than magnetic field. It's also important, that the spin-orbit coupling energy inside the wire should be much stronger than the the superconducting gap. However, there is a hope that this condition can generally be satisfied, as the proximitized superconductivity can be weakened by a proper fabrication process.

Chapter 6

Conclusion

In this work we have considered the system of two superconducting wires connected with a tunnel junction. A strong spin-orbit and a magnetic field perpendicular to the wire were assumed. The transparency of the barrier were set to be weak, so the system operates in tunneling regime. The model is introduced in detail in chapter 2.

The low-energy spectrum was obtained for different topological indexes of the wires. The subgap states, found in section 3.5, are quite predictable. In triv-top contact there is only one subgap state — a Majorana state, on zero energy, as it should be. In top-top contact there are two subgap states, which are Majorana states, each from its own wire. As there is a finite transparency of the barrier, these states are not at zero energy and demonstrate the energy splitting, calculated in section 3.5.2. In triv-triv contact there are no subgape states — this result, as well as the presence of only Majorana states in other contacts, wasn't obvious for us before, but also not especially surprising.

The supercurrent from low energy states was calculated in section 3.6. The main result is that it is expected be much smaller than the current from high energy states and probably won't be observable.

In chapter 4 the model was modified by introducing time dependent perturbation. Even the simple case, when gap in the trivial wire is much smaller than the gap in topological one and the ionization amplitude factorizes, demonstrates a rich physics with four different subregimes. The ionization rates for Majorana state for these subregimes were calculated, as well as the limits of applicability and their physical meaning is established.

Authors hope, that this work can give further incites for both developing experimental techniques of detecting Majorana states in 1D superconductors and theoretical studies of properties of such systems.

Appendix A

Wavefunctions for the stationary contact

Here the eigenstates of the junction are presented in leading and subleading order on the tunneling constant t. Only long-wave (ψ_{medium} and ψ_{longest}) part is presented here, as it's sufficient for chapter 4.

The states in Nambu-Gorkov space are written in bra-ket notation. For zero tunneling they are: $|\gamma_0\rangle$— the Majorana state and $|\varepsilon, L_0\rangle$, $|\varepsilon, R_0\rangle$ — continuous spectra in the left and in the right wire respectfully. The corrections are denoted as $|\gamma_1\rangle, |\varepsilon, L_1\rangle, |\varepsilon, R_1\rangle$.

It's important to note, that the first order correction for any state is located in the wire opposite to the one hosting the leading order. This can be reflected with spinors in LR-space as:

$$\Psi_\gamma = \begin{pmatrix} 0 \\ |\gamma_0\rangle \end{pmatrix}_{LR} + \begin{pmatrix} |\gamma_1\rangle \\ 0 \end{pmatrix}_{LR} + \dots \tag{A.1}$$

$$\Psi_R = \begin{pmatrix} 0 \\ |\varepsilon, R_0\rangle \end{pmatrix}_{LR} + \begin{pmatrix} |\varepsilon, R_1\rangle \\ 0 \end{pmatrix}_{LR} + \dots \tag{A.2}$$

$$\Psi_L = \begin{pmatrix} |\varepsilon, L_0\rangle \\ 0 \end{pmatrix}_{LR} + \begin{pmatrix} 0 \\ |\varepsilon, L_1\rangle \end{pmatrix}_{LR} + \dots \tag{A.3}$$

The states are normalized as:

$$\langle\gamma_0|\gamma_0\rangle = 1 \quad \langle\epsilon, R_0|\varepsilon, R_0\rangle = N_R(\epsilon)\,\delta(\epsilon - \varepsilon) \quad \langle\epsilon, L_0|\varepsilon, L_0\rangle = N_L(\epsilon)\,\delta(\epsilon - \varepsilon) \tag{A.4}$$

where

$$N_L(\varepsilon) = \frac{4\pi u \sqrt{\varepsilon^2 - g_L^2}\left(e^{2\kappa_L(\varepsilon)} + 1\right)^2}{\varepsilon} \quad N_R(\varepsilon) = \frac{4\pi u \sqrt{\varepsilon^2 - g_R^2}\left(e^{2\eta_R(\varepsilon)} + 1\right)^2}{\varepsilon} \tag{A.5}$$

Note, that for calculating s-matrix another normalization, providing $\langle\epsilon| v |\varepsilon\rangle = \delta(\epsilon - \epsilon)$ should be used, with $v = u\sigma_z\tau_z$ for long-wave states. The normalization used here serves for computing tunnel Hamiltonian matrix elements.

The definition of the $\eta_{L,R}$, η_L and κ_R is given in the 3.6. The indexes L, R near the spinors are relate to the wire, where this spinor is present. All the wavefucntions listed here are relevant

for both $|g_L| < g_R$ and $|g_L| > g_R$ cases.

The Majorana state is:

$$\langle x|\gamma_0 \rangle = \frac{1}{2}\sqrt{\frac{g_R}{u}} \begin{pmatrix} -1 \\ i \\ -i \\ 1 \end{pmatrix}_R e^{-\frac{g_R x}{u}} \tag{A.6}$$

$$\langle x|\gamma_1 \rangle = \frac{1}{2}\sqrt{\frac{g_R}{u}}\zeta t \left(e^{i\frac{\phi}{2}} + e^{-i\frac{\phi}{2}}\right) \left[\begin{pmatrix} -i \\ 1 \\ 1 \\ -i \end{pmatrix}_L e^{-\frac{2\Delta x}{u}} - i\zeta \begin{pmatrix} -i \\ -1 \\ 1 \\ i \end{pmatrix}_L e^{-\frac{|g_L| x}{u}} \right] \tag{A.7}$$

Continuous states from the right wire are:

$$\langle x|E, R_0\rangle =$$

$$\left(-ie^{\eta_R(E)} - 1\right) \begin{pmatrix} -1 \\ -e^{\eta_R(E)} \\ e^{\eta_R(E)} \\ 1 \end{pmatrix}_R e^{-\frac{ix\sqrt{E^2 - g_R^2}}{u}} + \left(e^{\eta_R(E)} + i\right) \begin{pmatrix} -e^{\eta_R(E)} \\ -1 \\ 1 \\ e^{\eta_R(E)} \end{pmatrix}_R e^{\frac{ix\sqrt{E^2 - g_R^2}}{u}} \tag{A.8}$$

$$\langle x|E\,R_1\rangle \Big|_{E<g_L} = t\zeta \left(e^{2\eta_R(E)} - 1\right)\left(e^{i\frac{\phi}{2}} + e^{-i\frac{\phi}{2}}\right) \times$$

$$\times \left[\begin{pmatrix} -i \\ 1 \\ 1 \\ -i \end{pmatrix}_L e^{-\frac{2\Delta x}{u}} - \frac{2i\zeta}{\left(1 + e^{-i\theta_L(E)}\right)} \begin{pmatrix} -ie^{-i\theta_L(E)} \\ -1 \\ 1 \\ ie^{-i\theta_L(E)} \end{pmatrix}_L e^{\frac{-x\sqrt{g_L^2 - E^2}}{u}} \right] \tag{A.9}$$

$$\langle x|E\,R_1\rangle \Big|_{E>g_L} = t\zeta \left(e^{2\eta_R(E)} - 1\right)\left(e^{i\frac{\phi}{2}} + e^{-i\frac{\phi}{2}}\right) \times$$

$$\times \left[\begin{pmatrix} -i \\ 1 \\ 1 \\ -i \end{pmatrix}_L e^{-\frac{2\Delta x}{u}} - \frac{2i\zeta}{\left(1 + ie^{-\kappa_l(E)}\right)} \begin{pmatrix} e^{-\kappa_L(E)} \\ -1 \\ 1 \\ -e^{-\kappa_L(E)} \end{pmatrix}_L e^{\frac{ix\sqrt{E^2 - g_L^2}}{u}} \right] \tag{A.10}$$

43

Continuous states from the left wire are:

$$\langle x | \varepsilon, L_0 \rangle =$$

$$\left(e^{\kappa_L(\varepsilon)} - i \right) \begin{pmatrix} 1 \\ -e^{\kappa_L(\varepsilon)} \\ e^{\kappa_L(\varepsilon)} \\ -1 \end{pmatrix}_L e^{+i \frac{\sqrt{\varepsilon^2 - g_L^2}}{u} x} + \left(-1 + i e^{\kappa_L(\varepsilon)} \right) \begin{pmatrix} e^{\kappa_L(\varepsilon)} \\ -1 \\ 1 \\ -e^{\kappa_L(\varepsilon)} \end{pmatrix}_L e^{-i \frac{\sqrt{\varepsilon^2 - g_L^2}}{u} x} \quad \text{(A.11)}$$

$$\langle x | \varepsilon, L_1 \rangle \Big|_{\varepsilon < g_R} = \zeta t \left(e^{2\kappa_L(\varepsilon)} - 1 \right) \left(e^{i\frac{\phi}{2}} + e^{-i\frac{\phi}{2}} \right) \times$$

$$\times \left[\frac{2i\zeta}{(-1 + e^{i\theta_R(\varepsilon)})} \begin{pmatrix} -1 \\ ie^{i\theta_R(\varepsilon)} \\ -ie^{i\theta_R(\varepsilon)} \\ 1 \end{pmatrix}_R e^{-x\frac{\sqrt{g_R^2 - \varepsilon^2}}{u}} + \begin{pmatrix} 1 \\ -i \\ -i \\ 1 \end{pmatrix}_R e^{-\frac{2\Delta x}{u}} \right] \quad \text{(A.12)}$$

$$\langle x | \varepsilon, L_1 \rangle \Big|_{\varepsilon > g_R} = \zeta t \left(e^{2\kappa_L(\varepsilon)} - 1 \right) \left(e^{i\frac{\phi}{2}} + e^{-i\frac{\phi}{2}} \right) \times$$

$$\times \left[\frac{2it\zeta}{(-1 + ie^{-\eta_R(\varepsilon)})} \begin{pmatrix} -1 \\ -e^{-\eta_R(\varepsilon)} \\ e^{-\eta_R(\varepsilon)} \\ 1 \end{pmatrix}_R e^{\frac{ix\sqrt{E^2 - g_R^2}}{u}} + \begin{pmatrix} 1 \\ -i \\ -i \\ 1 \end{pmatrix}_R e^{-\frac{2\Delta x}{u}} \right] \quad \text{(A.13)}$$

Appendix B

Tunnel Hamiltonian derivation

The goal in derivation tunnel Hamiltonian is to make it restoring the corrections of the wavefunctions from appendix A. Recalling, that in LR-space the Hamiltonian has the form (4.3), we write the unperturbed Green function as:

$$G_0\left(E\right) = \frac{1}{E+i0}\begin{pmatrix} 0 & 0 \\ 0 & |\gamma_0\rangle\langle\gamma_0| \end{pmatrix}_{LR} + \int_{g_L}^\infty \frac{d\varepsilon}{N_L\left(\varepsilon\right)}\frac{1}{E+i0-\varepsilon}\begin{pmatrix} |\varepsilon, L_0\rangle\langle\varepsilon, L_0| & 0 \\ 0 & 0 \end{pmatrix}_{LR} +$$
$$+ \int_{g_l}^\infty \frac{d\varepsilon}{N_R\left(\varepsilon\right)}\frac{1}{E+i0-\varepsilon}\begin{pmatrix} 0 & 0 \\ 0 & |\varepsilon, R_0\rangle\langle\varepsilon, R_0| \end{pmatrix}_{LR} \qquad \text{(B.1)}$$

with $N_{L,R}$ from (A.5). The corrections for the spinors should be calculated as:

$$\Psi_1\left(E\right) = G_0\left(E\right)H_T\Psi_0\left(E\right) \qquad \text{(B.2)}$$

So, for different states:

$$\left|\gamma_1\right\rangle = \int_{g_L}^\infty \frac{d\varepsilon}{N_L\left(\varepsilon\right)}\frac{1}{-\varepsilon+i0}\left|\varepsilon, L_0\right\rangle\left\langle\varepsilon, L_0\left|h_{LR}\right|\gamma_0\right\rangle \qquad \text{(B.3)}$$

$$\left|E+i0, R_1\right\rangle = \int_{g_L}^\infty \frac{d\varepsilon}{N_L\left(\varepsilon\right)}\frac{1}{E-\varepsilon+i0}\left|\varepsilon, L_0\right\rangle\left\langle\varepsilon, L_0\left|h_{LR}\right|E\,R_0\right\rangle \qquad \text{(B.4)}$$

$$\left|E+i0, L_1\right\rangle = \frac{1}{E+i0}\left|\gamma_0\right\rangle\left\langle\gamma_0\left|h_{LR}^\dagger\right|E, L_0\right\rangle +$$
$$+ \int_{g_l}^\infty \frac{d\varepsilon}{N_R\left(\varepsilon\right)}\frac{1}{E-\varepsilon+i0}\left|\varepsilon\,R_0\right\rangle\left\langle\varepsilon, R_0\left|h_{LR}^\dagger\right|E, L_0\right\rangle \qquad \text{(B.5)}$$

Now, multiplying the third equation by $\left\langle\gamma_0\right|$ and $\left\langle\epsilon, R_0\right|$, find:

$$\left\langle\gamma_0\left|E+i0, L_1\right\rangle = \frac{1}{E+i0}\left\langle\gamma_0\left|h_{LR}^\dagger\right|E, L_0\right\rangle \qquad \text{(B.6)}$$

$$\left\langle\epsilon, R_0\left|E+i0, L_1\right\rangle = \frac{1}{E-\epsilon+i0}\left\langle\epsilon, R_0\left|h_{LR}^\dagger\right|E, L_0\right\rangle \qquad \text{(B.7)}$$

The l.h.s. of this equation can be calculated with the help of appendix A. After doing so, we arrive to the result (4.5).

Appendix C

Multiphoton ionization

This appendix is focused on high-order perturbation theory, ionization rates in particular. In this Appendix Planck constant is taken to be unity.

C.1   Basics about Green's functions

The starting point is the general setup of a discrete bound state subject to a weak and slow perturbation $V(t)$. The bound state energy is zero. The goal is to obtain the ionization rate. The time evolution of the wave function obeys the Schroedinger equation:

$$i\frac{\partial}{\partial t}\Psi = (H_0 + V)\Psi \tag{C.1}$$

In the absence of perturbations, the solution is $\Psi(t) = \Psi_0$ (since $E_0 = 0$ it is literally time-independent). For further analysis it's convenient to consider the unperturbed retarded Green's function $G^R(E)$ defined so that:

$$G^R(E)(E + i0 - H_0) = 1 \tag{C.2}$$

If the bound state is normalized, $\langle\gamma|\gamma\rangle = 1$ and the continuous spectrum is normalized according to $\langle E|E'\rangle = N(E)\delta(E - E')$ with some reasonably nice $N(E)$ then:

$$\mathbb{I} = |\gamma\rangle\langle\gamma| + \int \frac{|E\rangle\langle E|}{N(E)}dE \tag{C.3}$$

Similarly, H_0 and G^R in the energy representation:

$$H_0 = \int \frac{|E\rangle\langle E|}{N(E)}EdE \qquad G^R(\epsilon) = \frac{|\gamma\rangle\langle\gamma|}{\epsilon + i0} + \int \frac{|E\rangle\langle E|}{(\epsilon + i0 - E)N(E)}dE \tag{C.4}$$

Integrals over E include all states in the continuous spectrum. Where the latter is degenerate, a summation over the degenerate states must be carried out. From now on the "R" index for retarded Green's function will be omitted.

In time representation the Green's function obeys:

$$\left(i\frac{\partial}{\partial t_2} - H_0\right)G(t_2, t_1) = \delta(t_2 - t_1) \tag{C.5}$$

One can formally introduce the Green's function in energy representation with two arguments as a Fourier-transform of $G(t_2, t_1)$:

$$G\left(E_2, E_1\right) = \iint e^{iE_2t_2 - iE_1t_1}G(t_2, t_1)dt_1dt_2 \tag{C.6}$$

As H_0 is time independent, $G\left(t_2, t_1\right) = G\left(t_2 - t_1, 0\right)$, so:

$$G\left(E_2, E_1\right) = 2\pi\delta\left(E_2 - E_1\right)G\left(E_1\right) \tag{C.7}$$

One can also find, that for any eigenstate $|E_0\rangle$

$$G\left(t\right)|E_0\rangle = -ie^{-iE_0t}\theta_H\left(t\right)|E_0\rangle \tag{C.8}$$

With the help of Green's function the Schroedinger equation (C.1) can be solved as:

$$\Psi(t) = \Psi_0 + \int G_0(t - t')V(t')\Psi_0(t')dt' +$$
$$\iint G_0(t - t')V(t')G_0(t' - t'')V(t'')\Psi_0(t'')dt'dt'' + \dots \tag{C.9}$$

where the Ψ_0 is unperturbed wavefunction. This equation can be rewriteen by the introducion

C.2   Fermi Golden Rule (first order)

Consider first the lowest order to the Fermi Golden rule by only keeping the linear term in V. Let the Fourier decomposition of V be:

$$V(t) = \sum_n V_n e^{-i\omega_n t} \tag{C.10}$$

(Hermiticity demands $V(t) = V(t)^*$ so that $V_n = V_{-n}^*$). Suppose there is an unperturbed continuous spectrum parameterized by E, with $\langle E|E'\rangle = f(E)\delta(E - E')$. The first step is to calculate

$\langle E|\Psi(t)\rangle$, i.e. the quantum amplitude of being in state $|E\rangle$ at time t. It is:

$$\langle E|\Psi(t)\rangle = \langle E|\int G_0(t-t')V(t')\Psi_0(t')dt'\rangle = \int \langle E|G_0(t-t')V(t')|\Psi_0\rangle dt' =$$

$$= \int\int \langle E|G_0(t-t')|E'\rangle\langle E'|V(t')|\Psi_0\rangle dt'\frac{dE'}{N(E)}$$

$$= \int e^{-i(t-t')E}\theta_H(t-t')\langle E|V(t')|\Psi_0\rangle dt' =$$

$$= e^{-iEt}\sum_n\int e^{it'(E-\omega_n)}\theta_H(t-t')\langle E|V_n|\Psi_0\rangle dt' \quad\text{(C.11)}$$

Assuming that the perturbation was turned on at $t' = 0$ the integral over t' is taken from t_0 to t and gives:

$$\langle E|\Psi(t)\rangle = e^{-iEt}\sum_n\langle E|V_n|\Psi_0\rangle\frac{e^{it(E-\omega)}-1}{i(E-\omega_n)} \quad\text{(C.12)}$$

Thus, the probability density of being in the state $|E\rangle$ is (omit all frequencies except the resonant on should be ommited since the contributions from non-resonant frequencies can be neglected at long times):

$$\rho(E) = |\langle E|V_n|\Psi_0\rangle|^2\frac{4\sin^2\frac{t(E-\omega_n)}{2}}{(E-\omega_n)^2} \quad\text{(C.13)}$$

so that the probability of being in a state between E and $E+\delta E$ is at large times:

$$P(E+\delta E, E) = |\langle E|V_n|\Psi_0\rangle|^2\int\limits_E^{E+\delta E}\frac{dE}{N(E)}\frac{4\sin^2\frac{t(E-\omega_n)}{2}}{(E-\omega_n)^2} =$$

$$= 2t|\langle E|V_n|\Psi_0\rangle|^2\int\limits_E^{E+\delta E}\frac{d(tE/2)}{N(E)}\frac{4\sin^2\frac{t(E-\omega_n)}{2}}{t^2(E-\omega_n)^2} =$$

$$= 2t|\langle E|V_n|\Psi_0\rangle|^2\frac{\pi}{N(E)}\theta_H(\omega_n-E)\theta_H(E+\delta E-\omega_n) \quad\text{(C.14)}$$

In other words, the probability density at large t behaves exactly like the δ-function:

$$\rho(E) = 2\pi|\langle E|V_n|\Psi_0\rangle|^2\delta(E-\omega_n) \quad\text{(C.15)}$$

which is the well-known Fermi Golden rule. (Note, that the probability is $dP = \rho(E)dE/f(E) -$ do not forget the normalization). Thus, the ionization rate (i.e. P/t) for a single photon is expressed

as:

$$\mathcal{I} = \frac{2\pi |\langle E|V_n|\Psi_0\rangle|^2}{N(E)} \tag{C.16}$$

C.3 Fermi Golden Rule (high order)

Tho treat the higher-order perturbation theory it's convenient to rewrite (C.9) as:

$$\Psi(t) = \Psi_0 + \int\int G_0(t-t')W(t',t'')\Psi_0(t'')dt'dt'' \tag{C.17}$$

where W incorporates all powers of perturbation theory:

$$W = V + VG_0V + VG_0VG_0V + \ldots \tag{C.18}$$

The perturbation V in energy space is:

$$V(E', E) \equiv \int V(t', t)e^{it'E' - iEt}dt'dt = \int V(t)e^{i(E'-E)t}dt =$$

$$= \sum_n V_n \int e^{i(E'-E-\omega_n)t}dt = \sum_n V_n 2\pi\delta(E' - E - \omega_n) \tag{C.19}$$

The second term of the perturbation theory $W_2 = VGV$ in energy representation reads:

$$W_2(E_2, E_1) = \int V(E_2, E)G_0(E, E')V(E', E_1)\frac{dEdE'}{(2\pi)^2} =$$

$$\sum_{nm} 2\pi\delta(E_2 - E_1 - \omega_n - \omega_m)V_nG_0(E_1 + \omega_m)V_m \tag{C.20}$$

Very similarly, the N-th-order term is:

$$W_N(E_2, E_1) = \sum_{n_1,\ldots,n_N} 2\pi\delta\left(E_2 - E_1 - \sum_{i=1}^{N}\omega_{n_i}\right)V_{n_N}\prod_{j=1}^{N-1}G_0\left(E_1 + \sum_{s=1}^{j}\omega_{n_s}\right)V_{n_j} \tag{C.21}$$

The above expression sums over all processes involving N photons. Note how the Green's functions contains the cumulative energy of all photons absorbed by the time. The δ-function at the start of the expression indicates that the energy is changed by $\sum \omega_{n_i}$. It makes more sense to sort processes within W not by photon count N but rather by the total energy gained, since the total ionization rate should be dominated by ionization to the lowest accessible continuum state.

Defining this activation energy as $\mathcal{E}$, write:

$$W_{\mathcal{E}}(E_2, E_1) = 2\pi\delta(E_2 - E_1 - \mathcal{E})w_{\mathcal{E}}(E_1) \tag{C.22}$$

$$w_{\mathcal{E}}(E) = \sum_{\{n_i\}:\mathcal{E}} V_{n_N} \prod_{j=1}^{N-1} G_0\left(E + \sum_{s=1}^{j} \omega_{n_s}\right) V_{n_j} \tag{C.23}$$

The summation is over all sets of photons n_i that total an energy of $\mathcal{E}$, i.e. such sets that $\sum_i^N \omega_{n_i} = \mathcal{E}$. The photon number N itself depends on the particular photon set n_i. The total composite perturbation W can be written as a sum of $W_{\mathcal{E}}$ with different $\mathcal{E}$. However, only one term is relevant — the one with $\mathcal{E} = \min |g_R|, |g_L|$. (If the elementary frequency quantum ω is large enough, this is replaced by the lowest $\mathcal{E}$ that surpasses the minimum gap).

Now the Fermi Golden rule result (C.16) can be rederived for $W_{\mathcal{E}}$. It's easy ti see that W has the same energy structure as the single-photon perturbation V. Both operators simply shift the energy. Thus, one may simply put $W_{\mathcal{E}}$ into the Fermi Golden rule instead of V to get the full-theory results:

$$\mathcal{I} = \frac{2\pi|\langle\mathcal{E}|w_{\mathcal{E}}|\Psi_0\rangle|^2}{N(\mathcal{E})} \tag{C.24}$$

Thus to find the ionization rate one should calculate $w_{\mathcal{E}}$ from (4.10).

Bibliography

[1] E. Majorana, "Teoria simmetrica dell'elettrone e del positrone", Il Nuovo Cimento (1937).

[2] S. R. E. Frank T. Avignone and and J. Engel, "Double beta decay, majorana neutrinos, and neutrino mass", Rev. Mod. Phys. **80**.

[3] A. Giuliani and A. Poves, "Neutrinoless double-beta decay", Advances in High Energy Physics **2012**.

[4] S. Dell'Oro, S. Marcocci, M. Viel, and F. Vissani, "Neutrinoless double beta decay: 2015 review", Advances in High Energy Physics **27** (2016).

[5] R.Jackiw and P.Rossi, "Zero modes of the vortex-fermion system", Nuclear Physics B **190** (1981).

[6] A. Y. Kitaev, "Unpaired majorana fermions in quantum wires", Uspekhi Fizicheskikh Nauk **44** (2001).

[7] N. B. Kopnin and M. M. Salomaa, "Mutual friction in superfluid $\mathcal{H}]^3$: effects of bound states in the vortex core", Phys. Rev. B **44** (1991).

[8] O. Motrunich, K. Damle, and D. A. Huse, "Griffiths effects and quantum critical points in dirty superconductors without spin-rotation invariance: one-dimensional examples", Phys. Rev. B **63** (2001).

[9] S. D. Sarma, C. Nayak, and S. Tewari, "Proposal to stabilize and detect half-quantum vortices in strontium ruthenate thin films: Non-Abelian braiding statistics of vortices in a $p_x + ip_y$ superconductor", Phys. Rev. B **73** (2006).

[10] N. Read and D. Green, "Paired states of fermions in two dimensions with breaking of parity and time-reversal symmetries and the fractional quantum hall effect", Phys. Rev. B **61** (2000).

[11] T. Senthil and M. P. A. Fisher, "Quasiparticle localization in superconductors with spin-orbit scattering", Phys. Rev. B **61** (2000).

[12] G. Volovik, "Fermion zero modes on vortices in chiral superconductors", Pisma Zh.Eksp.Teor.Fiz. **70** (1999).

[13] L. Fu and C. L. Kane, "Superconducting proximity effect and majorana fermions at the surface of a topological insulator", Phys. Rev. Lett. **100** (2008).

[14] R. Aguado, "Majorana quasiparticles in condensed matter", La Rivista del Nuovo Cimento **40** (2018).

[15] C. W. J. Beenakker, "Search for majorana fermions in superconductors", Annu. Rev. Con. Mat. Phys. **4** (2013).

[16] F. von Oppen, Y. Peng, and F. Pientka, *Topological superconducting phases in one dimension* (2014).

[17] C. Chamon, R. Jackiw, Y. Nishida, S.-Y. Pi, and L. Santos, "Quantizing majorana fermions in a superconductor", Phys. Rev. B **81** (2010).

[18] S. R. Elliott and M. Franz, "Colloquium: majorana fermions in nuclear, particle, and solid-state physics", Rev. Mod. Phys. **87** (2015).

[19] J. Alicea, Y. Oreg, G. Refael, F. von Oppen, and M. P. A. Fisher, "Non-abelian statistics and topological quantum information processing in 1d wire networks", Nature Physics **7** (2011).

[20] C. Nayak, S. H. Simona, M. F. Ady Stern, and S. D. Sarma, "Non-abelian anyons and topological quantum computation", Rev. Mod. Phys. **80** (2008).

[21] A. Romito, J. Alicea, G. Refael, and F. von Oppen, "Manipulating majorana fermions using supercurrents", Phys. Rev. B **85** (2012).

[22] V. Mourik, K. Zuo1, S. M. Frolov, S. R. Plissard, E. P.A. M. Bakkers, and L. P. Kouwenhoven, "Signatures of majorana fermions in hybrid superconductor-semiconductor nanowire devices", Science **336** (2012).

[23] S. Vaitiekėnas, M.-T. Deng, P. Krogstrup, and C. M. Marcus, "Flux-induced majorana modes in full-shell nanowires", arXiv:1809.05513 (2018).

[24] H. Zhang, C.-X. Liu, S. Gazibegovic, D. Xu, J. A. Logan, G. Wang, N. van Loo, J. D. S. Bommer, M. W. A. de Moor, D. Car, R. L.M. O. het Veld, P. J. van Veldhoven, S. Koelling, M. A. Verheijen, M. Pendharkar, D. J. Pennachio, B. Shojaei, J. S. Lee, C. J. Palmstrøm, E. P.A. M. Bakkers, S. D. Sarma, and L. P. Kouwenhoven, "Quantized majorana conductance", Nature **556** (2018).

[25] Y. Oreg, G. Refael, and F. von Oppen, "Helical liquids and majorana bound states in quantum wires", Phys. Rev. Lett. **105** (2010).

[26] R. Lutchyn, J. Sau, and D. Sarma, "Majorana fermions and a topological phase transition in semiconductor-superconductor heterostructures", Phys. Rev. Lett. **105** (2010).

[27] C. Beenakker, "Three "universal"mesoscopic josephson effects", Transport Phenomena in Mesoscopic Systems **109**, 235–253 (2004).

[28] E. Akkermans, A. Auerbach, J. E. Avron, and B. Shapiro, "Relation between persistent currents and the scattering matrix", Physical Review Letters **66**, 76 (1991).